THE PENNSYLVANIA STATE UNIVERSITY
SCHREYER HONORS COLLEGE

THE SCHOOL OF ENGINEERING DESIGN, TECHNOLOGY,
AND PROFESSIONAL PROGRAMS

A TECHNO-ECONOMIC ANALYSIS OF THE POTENTIAL FOR
SALINITY GRADIENT POWER GENERATION IN THE GAMBIA

DAVID RICHARD HUGHES
SPRING 2015

A thesis
submitted in partial fulfillment
of the requirements
for a baccalaureate degree
in Chemical Engineering
with honors in Engineering Leadership Development

Reviewed and approved* by the following:

Andrew Zydney
Distinguished Professor of Chemical Engineering
Thesis Supervisor

Andrew M. (Mike) Erdman
Walter L. Robb Director of Engineering Leadership Development
Honors Adviser

* Signatures are on file in the Schreyer Honors College.

i

ABSTRACT

As fresh river water flows into the sea, chemical potential energy is dissipated during the mixing process due to the large difference in salt concentration between these waters. It is possible to extract some of this chemical potential energy as useful work, offering the possibility of a reliable, local, renewable source of energy. The Gambia is a developing country on the coast of West Africa that is centered geographically, culturally, and historically on the Gambia River. Salinity gradient power using flow from the Gambia River could provide an attractive option as the Gambia looks to expand electricity generation capacity.

A high-level technological and economic analysis of the production of electrical power using pressure retarded osmosis (PRO) was conducted to understand the short-term and long-term viability of this process for energy generation in the Gambia. Current membrane technology was modeled and a sensitivity analysis was carried out on key variables to determine the effects of possible future technological improvements.

The short-term viability of this technology, both in the Gambia and in other regions around the world, is limited mainly by the current market landscape and the economics of the PRO process based on current membrane technology and prices. Membrane cost, membrane life, and water permeability are the key drivers that make the current technology more expensive than alternative energy sources. The long-term viability of PRO technology in the Gambia would also be limited by access to water with a sufficiently low salt concentration as saline water intrusion is significant in the Gambia River estuary.

At this point, the capital investment for a PRO plant would likely be better spent investigating alternative energy generation technologies to provide reliable access to electricity for the Gambian people, but improvements in membrane cost and performance or changes in market conditions could make PRO an attractive option at some point in the future.

TABLE OF CONTENTS

LIST OF FIGURES

LIST OF TABLES

ACKNOWLEDGEMENTS

Chapter 1

Introduction to the Gambia

The Gambia is a country located on the coast of West Africa, bordered on the west by the Atlantic Ocean and on all other sides by Senegal. With an area less than the size of the state of Connecticut, it is the smallest country on the African mainland. A long, narrow country that extends approximately 400 km inland, the geography of the country is dominated by the Gambia River, which flows through the center of the country. As of 2014, the population is approximately 1.8 million people and growing at a rate of 2.7% per year [1].

Figure 1. Map of the Gambia showing Gambia River basin [2]

1.1 Historical Context

Humans have been living on the banks of the Gambia River for thousands of years. For most of this time, civilization has consisted of agricultural communities based in the fertile floodplain of the Gambia River. The Portuguese were the first Europeans to reach the Gambia River in 1455, and over the next two hundred years they traded extensively in salt, guns, ivory, gold, and slaves [3]. By 1650, the Portuguese were ousted by French and British forces, who competed for control of the region until the Peace of Paris in 1783 [3]. Under this agreement, Britain surrendered the land that would become Senegal to France in exchange for maintaining control over the Gambia River region. The British continued to rule the region until 1965, when the Gambia gained its independence from Britain in the post-World War II period of decolonization. In 1970, the Gambia successfully held a referendum to become a republic under the leadership of Dawda Kairaba Jawara. Jawara was reelected five times and held power until July of 1994, when Yahya Jammeh took power in a military coup.

1.2 Current Socioeconomic Status

The population of the Gambia struggles with poverty, with 48.4% of the population below the poverty line; average income in the country is approximately $500 per person per year [1]. The Gambia ranks number 172 out of 187 countries and territories in the 2014 United Nations Human Development Index Report, which assesses long-term progress in life expectancy, education, and economic standard of living [4]. The country's GDP has grown at an average rate of 3.6% per year over the past ten years and is forecasted to grow at 4.9% per year

over the next three years [1]. Nearly 75% of the population of the Gambia is employed in agriculture, which accounts for 25% of the country's GDP and 70% of the domestic exports [5]. Most agricultural production is centered on subsistence crops and cash crops such as cashews, peanuts, and cotton [6]. In addition to agriculture, the tourism and service sector is the major economic driver for the Gambia, accounting for 60% of the GDP [5]. Although the government has attempted to promote the manufacturing sector, it only accounts for about 5% of the GDP and growth is stagnant. Growth and investment in the economy, especially the manufacturing sector, has been impeded by lack of reliable and economically available energy.

1.3 Energy Landscape: Supply and Demand

Improvements in the quality and quantity of energy services in the Gambia are necessary to meet economic and social development needs [5]. Currently, more than 90% of Gambians rely on wood and other traditional biomass to meet basic energy needs including cooking and heating [5]. There are significant costs associated with heavy reliance on biomass including poor fuel quality and efficiency, detrimental health effects, and the large amount of time spent gathering fuel. Only 35% of Gambians have access to electricity [5]. As a result, Gambians consume only 136 kWh of electricity per person per year, versus the African average consumption of 575 kWh, the global average consumption of 2,770 kWh, and the United States average consumption of 10,837 kWh [5, 7].

The National Water & Electricity Company, Ltd. (NAWEC) is currently the main utility supplier for the Gambia. The majority of electricity is produced in the Greater Banjul Area

(GBA) by the Kotu Power Station (current capacity of 27.2 MW, nameplate capacity of 41.4 MW) [8]. This station consists of two light fuel oil (LFO) and seven heavy fuel oil (HFO) engines that power the generators [8]. The Brikama 2 Power Station (BPS2) was commissioned in July 2011 with a 9 MW capacity and has also been providing power to the GBA [8]. BPS2 Phase II plans are currently underway to add another 20 MW of generation capacity; funding is being provided by the International Development Bank [9]. Outside the GBA, there are seven provincial power stations that provide electricity to the more rural areas of the country. Currently, electricity is generated using diesel engines which run for 6 hours in the morning and 6 hours in the evenings [10]. A $20 million Phase II Expansion project is planned which will install two HFO powered generators (2.7 MW and 2.9 MW) in Farafenni and Basse, respectively [9]. According to NAWEC, this will be the first time that HFO generators will be installed in rural Gambia, with the goal of ensuring round-the-clock electricity supply [9].

Table 1. Rural power generation capacity in the Gambia [10]

Town	Installed Capacity (kW)
Basse	1950
Barra	480
Bansang	750
Farafenni	1750
Mansakonko	625
Kerrewan	220
Kaur	180

The only major power transmission and distribution network in the Gambia is in the GBA, which consists of three 33 kV feeders and five 11 kV feeders. The 33 kV lines supply substations which transform the voltage to 11 kV for further distribution [10]. Low voltage transformer substations then distribute three-phase 400 V electricity and single-phase 230 V to consumers [8]. The existing distribution infrastructure, rather than the available generation capacity from the GBA/Brikama power stations, is often the limiting factor determining the amount of power that can be distributed to consumers [11]. Network reliability is poor due to obsolete and overloaded equipment as well as the physical proximity to the ocean—the salt-laden air lowers the dielectric strength of insulators and affects the mechanical integrity of the hardware [11]. In rural areas, NAWEC has built other small distribution networks surrounding the rural power stations. However, there is no national electricity transmission backbone as these networks are unconnected to the main GBA network.
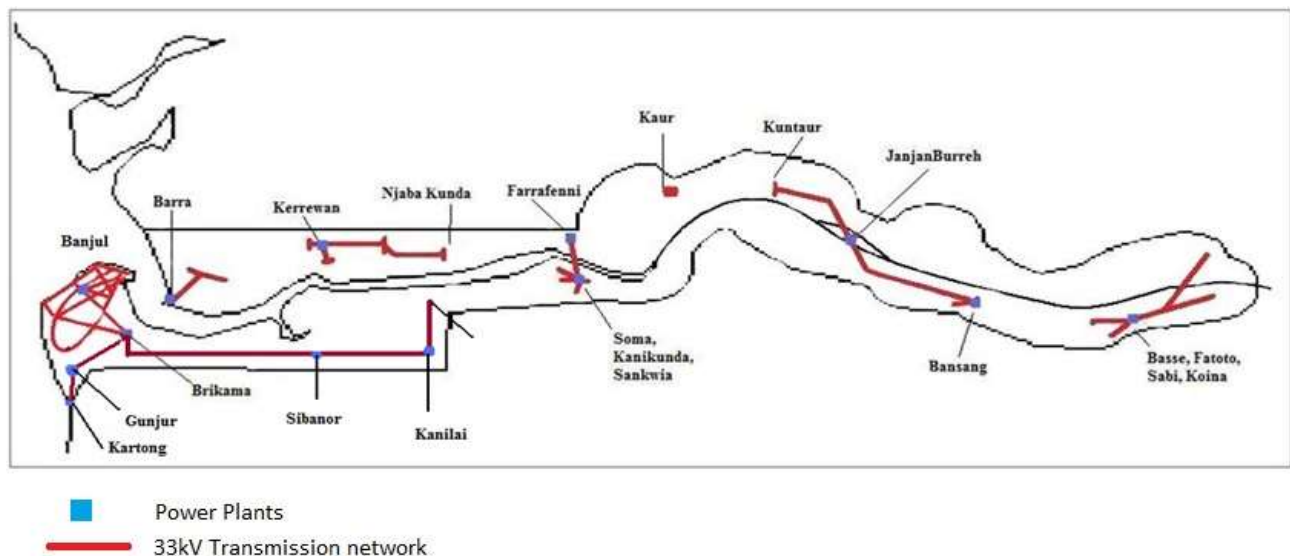
Figure 2: Gambian power transmission and distribution network [10]

The Gambia Public Utilities Regulatory Authority (PURA) provides government oversight and regulation for electricity, water, transportation, and telecommunications. Prior to 2005, the NAWEC held a monopoly on power generation, transmission, and distribution. With the passing of the Electricity Act of 2005, the Gambia provided a legal framework for private enterprises to generate and distribute electricity to the public [12]. By doing this, the government hoped to stimulate private sector investment in electricity generation and distribution and to control prices through competition. Since then, there have been three independent power producers join NAWEC as electricity generators. First, the Global Electric Company has operated the 25 MW Brikama Power Station 1 (BPS1) since 2006 using HFO engines [10]. Second, the GAMWIND company has operated the 900 kW Tanji Wind Park since 2012 [10]. Finally, the village of Batakunku uses a 150 kW wind turbine to produce electricity [10].

Current electricity prices are given in the table below, based on an assumed exchange rate of US $1 = 35 Gambian dalasi. For comparison, the average price for electricity in the USA for all sectors in 2012 was 9.84 cents/kWh [7].

Table 2. Gambian electricity prices by category [13]

Category	Price ($/kWh)
Domestic (prepaid)	0.26
Commercial	0.28
Hotel/Club/Industries * VAT included	0.34
Agriculture	0.26
Government	0.28

1.4 Future Outlook

In the coming years, the expansion of reliable electricity service to Gambian citizens will continue to be a high priority for the Gambian government. The government is working to expand infrastructure in order to release pent-up consumer demand and to encourage economic growth and development. A 2012 report co-published by the Gambian Ministry of Finance & Economic Affairs and the foreign aid office of the European Union cites unreliable, expensive, and limited electricity as one of the most critical factors constraining the business environment [14]. In addition to the commercial sector, the private population contributes to the rising demand for electricity due to the rapid urbanization of the country and the desire of the population for continued improvements in quality of life. However, demand has been suppressed by the current limitations on generation, transmission, and distribution of electric power. Currently, the total electricity generation capacity is approximately 68 MW. In order to raise the country to the current average for African electricity consumption, a capacity of at least 118 MW is required. To meet the global average electricity consumption level, a capacity of at least 569 MW is required. This number will continue to increase as both the Gambian population grows and average electricity usage rises.

At present the overwhelming majority of electricity is generated using non-renewable energy sources such as fuel oil and diesel. This means that the cost of generating electricity is heavily dependent on the global market for these products. In an effort to reduce this dependency as well as to preserve the environment, the Gambian government is committed to developing renewable energy sources to meet the country's future energy challenges. Along with Senegal, Guinea, and Guinea-Bissau, the Gambia is a member of the Gambia River Basin Development Organization (OMVG), which intends to develop hydropower from the

Sambangalou Dam project on the Gambia River. The dam will be located upstream of the Gambia in Senegal and will provide the Gambia with 40 MW starting in 2018 [14]. In 2013, the government passed the Renewable Energy Act which exempts renewable energy projects from import, corporate, and value-added taxes for fifteen years from commissioning [15]. Furthermore, the Act creates an electricity tariff subsidy and creates a Renewable Energy Fund which is used to incentivize the use of renewable technologies [15]. The European Union has also provided support for the application of renewable energy technologies in the Gambia.

Significant challenges exist for the development of renewable energy in the Gambia today. Managing the high start-up costs of renewable energy projects is often difficult because financing for these types of projects is expensive and challenging to acquire. Finding skilled workers to support the projects is also very difficult due to the overall low level of educational achievement in the country and the lack of technical and vocational skills. Despite these challenges, substantial opportunities exist that would enable the Gambia to meet its long-term development goals for renewable energy production.

Chapter 2

Introduction to Salinity Gradient Power

Although it is less widely known and publicized than wind or solar, salinity gradient power has potential as a source of renewable energy in the Gambia. Typically, rivers are considered to be sources of hydroelectric power, in which the gravitational potential energy of the river is harnessed as it flows down the elevation gradient towards its final destination, e.g. through the use of water-powered turbines. In addition to gravitational potential energy, rivers that flow into the ocean have vast chemical potential energy as a result of the salinity gradient (difference in salt concentration) between the fresh river water and the saline water of the ocean. According to Norman, "The energy flux available for natural salination is equivalent to each river in the world ending at its mouth in a waterfall 225 meters high" [16]. For comparison, the Hoover Dam is 221 meters (726 feet) tall [17]. Currently, this energy is simply dissipated as the river and the ocean waters mix at the mouth of the river. However, if this mixing were to occur in a controlled manner, it is possible to extract useful work in the form of electrical energy. In principle, this would provide a plentiful, renewable, and environmentally friendly source of energy.

The Gambia River dominates both the landscape and history of the Gambia. Most of the Gambia is a flat floodplain with limited potential for hydroelectric power generation; the average elevation gradient is only 0.002 m/km [18]. Only a few places in the country exceed 50 m in elevation [19]. However, the salinity gradient of the Gambia River as it flows into the Atlantic Ocean could provide a continuous, reliable, and local source of electricity for the Gambian

people. Not only would this reduce the dependency of the Gambia on imported petroleum energy sources, on which it is almost completely reliant today, it would also provide a geographically strategic source of energy. As most of the population and demand for energy in the Gambia is concentrated in and around the capital city of Banjul on the west coast (near the Atlantic Ocean), a salinity gradient power plant built near the mouth of the Gambia River would be well situated to satisfy the major energy needs of the country with minimal requirements for long-range transmission and distribution infrastructure.

2.1 Thermodynamic Basis for Salinity Gradient Power

When a dilute salt solution such as river water mixes with a more concentrated salt solution such as seawater, the chemical potential energy gradient causes spontaneous, irreversible mixing of the two solutions. In the case of a river estuary, the mixing of the river effluent and seawater occurs due to this chemical potential energy gradient as well as mass exchange due to the flow of the river. If the mixing of the two solutions can be achieved through a controlled process, it is possible to extract some of this chemical potential energy as useful work. The theoretical amount of energy available for extraction from the mixing process is given by the Gibbs free energy of mixing, ΔG_{mix}.
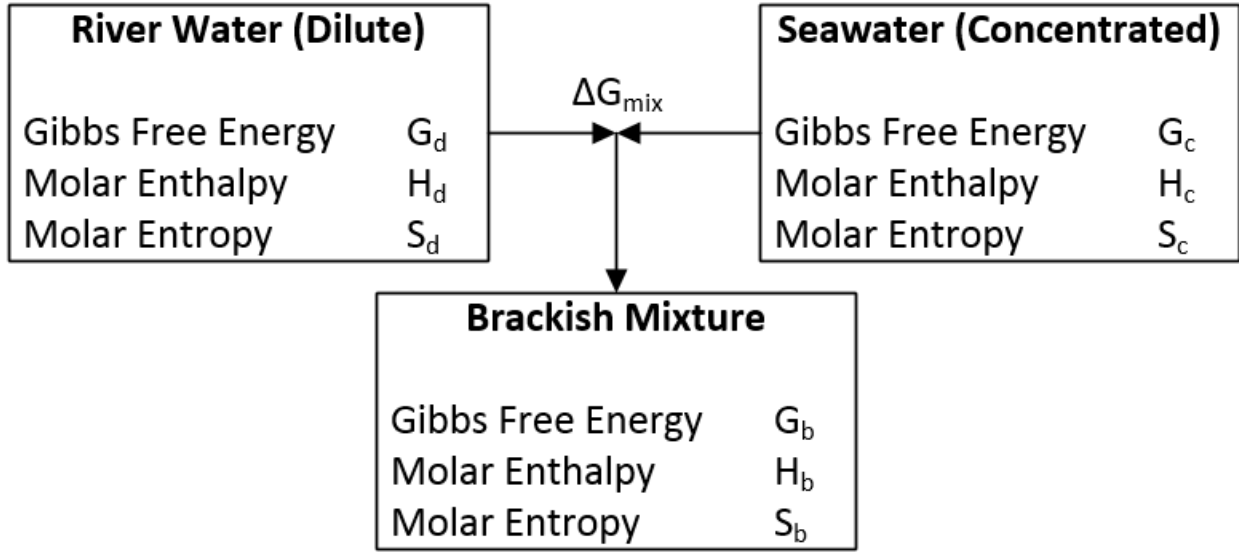
Figure 3: Thermodynamic parameters of natural salination

For ideal solutions, the Gibbs free energy of mixing is given by Equation (1), where G indicates the Gibbs free energy of the solution, the subscript c indicates the concentrated solution (seawater), the subscript d indicates the dilute solution (fresh water), and the subscript b indicates the brackish water solution that is produced when the two feed solutions are mixed [20].

$$\Delta G_{mix} = G_b - (G_c + G_d) \qquad [1]$$

The expression for the Gibbs free energy of each solution can be substituted into Equation (1) to provide the following expression (assuming $\Delta H_{mix} = 0$ as for an ideal solution):

$$\Delta G_{mix} = -(n_c + n_d)\, T\, \Delta S_{mix,b} + \left(n_c\, T\, \Delta S_{mix,c} + n_d\, T\, \Delta S_{mix,d}\right) \qquad [2]$$

where T is the temperature, n is the number of moles, and ΔS_{mix} is the molar entropy of mixing for each solution. The molar entropy of mixing for an ideal solution is given by Equation (3):

$$\Delta S_{mix} = -R \sum_i x_i \ln x_i \qquad [3]$$

where R is the ideal gas constant and x is the mole fraction of component i. According to Equations (2) and (3), the theoretically available amount of energy from mixing fresh water

(~1.5 mM or 88 mg/L NaCl) in an infinite reservoir of seawater (~600 mM or 35 g/L NaCl) is

2.76 MJ/m^3 of fresh water [21]. Note that this is also the minimum energy required for

desalination of seawater to produce fresh (drinking) water.

There are currently two leading technologies available that can transform the chemical

potential energy of salination into useful work: pressure retarded osmosis (PRO) and reverse

electrodialysis (RED). The following two sections provide an overview of each technique

focusing on the key physical principles that govern the extraction of useful energy.

2.2 Overview of Pressure Retarded Osmosis

Osmosis is the process that occurs when two solutions of different solute (e.g., salt)

concentrations are separated by a semipermeable membrane. If the membrane is permeable to

the solvent but not the solute, the solvent will tend to spontaneously diffuse across the membrane

from the less concentrated side to the more concentrated side as shown in Figure 4. In the case

of a Gambian PRO plant, the dilute solution would be river water and the concentrated solution

would be seawater, with water as the solvent and salt as the solute.
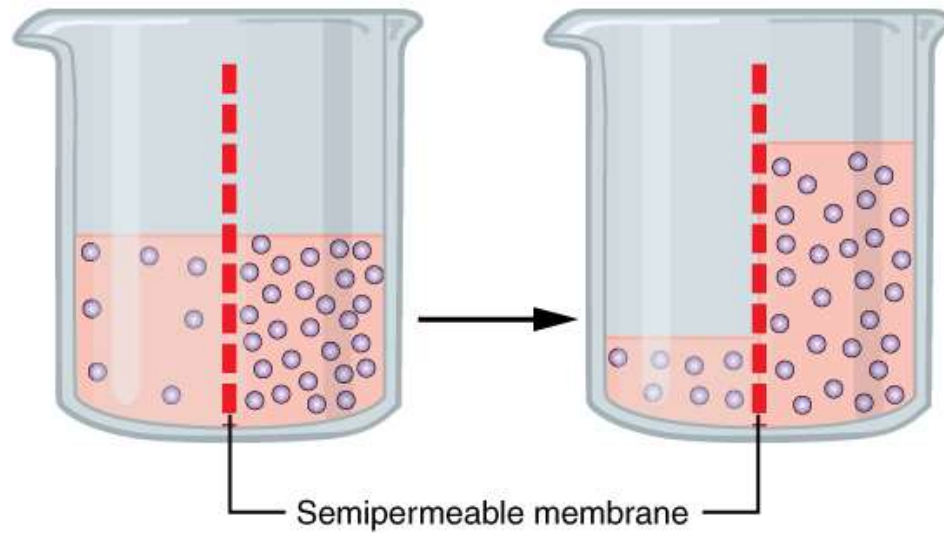
Figure 4: Process of osmosis [22]

The process of osmosis occurs spontaneously and does not, in and of itself, generate any useful energy. However, pressure can be applied to the concentrated solution side to impede the movement of the solvent by osmosis. The pressure which must be applied to completely stop the osmotic flow is called the osmotic pressure, π. For an ideal solution, the osmotic pressure is given by the Morse equation [23]:

$$\pi = iMRT \qquad [4]$$

where i is the dimensionless van't Hoff factor, M is the molarity of the solution, R is the ideal gas constant, and T is the absolute temperature. In the absence of an applied pressure, the osmotic flow will stop when the hydrostatic pressure from the increased fluid level on one side of the membrane is equal to the osmotic pressure difference as shown in Figure 4.

Salinity gradient energy can be harnessed to generate power through PRO based on the energy stored in the pressurized solution. In this application, a low-pressure fresh water stream, called the "feed" stream, is brought in contact with a high-pressure saline stream, called the

"draw" stream, in adjacent chambers of a membrane module. Water is transported across the membrane, which increases the volume of water on the high-pressure draw side. This pressurized stream is then used to drive a turbine and generate power. An idealized version of the system is shown in Figure 5.

Feed Pump Power Input: $W_{in} = V_s \Delta P$
Turbine Power Delivered: $W_{out} = (V_s + \Delta V) \Delta P$
Net Power Generated: $W_{net} = \Delta V * \Delta P$
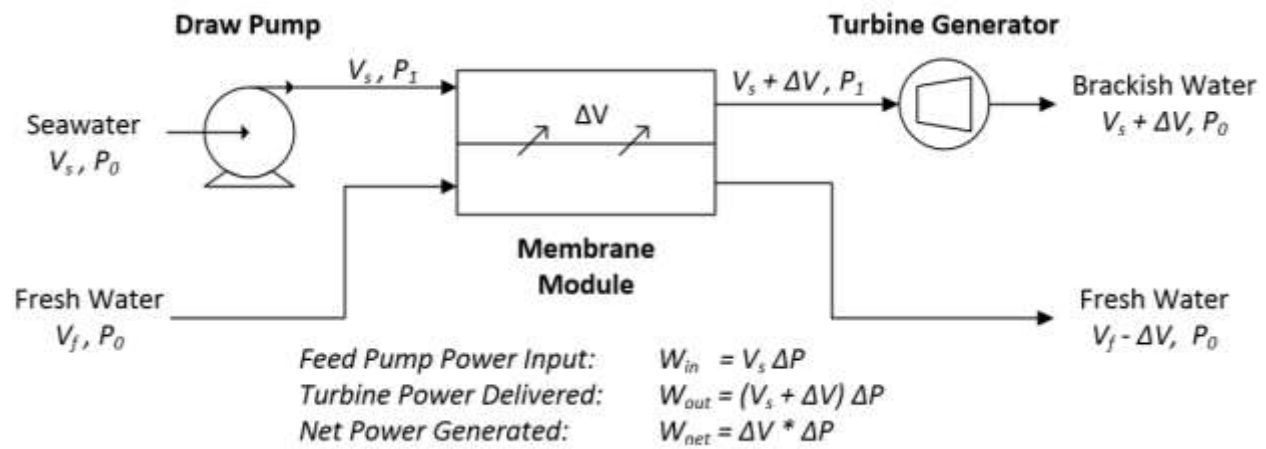
Figure 5: Idealized PRO system - Adapted from [24]

In this example, a seawater stream and a fresh water stream enter at pressure P_0 and with volumetric flow rates V_s and V_f, respectively. The seawater stream is pressurized by the draw pump to the operating pressure P_1 and enters the membrane module, while the fresh water enters the module at its original pressure P_0. Water is transported across the membrane by osmosis, creating brackish water at pressure P_1 with a flow rate that is greater than that of the initial seawater. This stream enters the turbine generator, where energy is extracted as the pressure is reduced back to the initial pressure, P_0. Assuming 100% efficiency for all rotating equipment and no friction losses, the net power that is generated from this system is given by the volume of water transported across the membrane multiplied by the difference in pressures:

$$W_{net} = W_{out} - W_{in} = \Delta V * \Delta P \qquad [5]$$

The key to power generation in pressure retarded osmosis is that the energy required to pressurize the seawater is less than the energy that can be extracted from the brackish water due to the greater flow rate of the brackish water stream.

To maximize the instantaneous power output of the system, the ideal operating pressure P_1 can be shown to be equal to one-half of the osmotic pressure differential, $\Delta\pi$ —the pressure must be higher than P_0, but any higher than $\Delta\pi/2$ causes an incremental decrease in flux that more than offsets the incremental gain from a higher operating pressure [24]. For a river water – seawater setup, the osmotic pressure differential is about 26 bar, so the ideal operating pressure would be about 13 bar (190 psi) [24]. To maximize power output over time, the operating pressure would decrease as water is transported across the membrane and the osmotic power differential decreases due to dilution of the draw solution and concentration of the feed solution. In actual PRO systems, the optimal operating pressure also depends on the membrane characteristics, which is a current topic of research [25].

The volumetric flow through the membrane (ΔV) is a function of the osmotic pressure difference ($\Delta\pi$), the difference in pressures between the seawater and fresh water (ΔP), the membrane area (A), and the permeability coefficient of the membrane (k_p):

$$\Delta V = k_p \, A \, (\Delta\pi - \Delta P) \qquad [6]$$

The overall expression for the power generation capability for an idealized PRO system is given by Equation (7), which simplifies to Equation (8) if it is assumed that ΔP is equal to the ideal operating pressure. Note that in this idealized system, the amount of fresh water transported across the membrane is assumed to be very small in relation to the total seawater flow, with the net result that $\Delta\pi$ is constant at the value given by the relative salinity of the inlet streams, i.e.,

there is no dilution of the seawater by the flux of fresh water. In an actual PRO system, the

power generation capability will decrease as $\Delta\pi$ changes due to water transport.

$$W_{net} = \ k_p \ A \ \Delta P \ (\Delta\pi - \Delta P) \qquad\qquad [7]$$

$$W_{net} = \ k_p \ A \frac{\Delta\pi^2}{4} \qquad\qquad [8]$$

According to Equation (7), the key variables for determining the power generated from a PRO

system are the osmotic pressure, the operating pressure, the permeability coefficient, and the

membrane area. Additional practical and economic considerations must be accounted for in the

design and implementation of an actual system; these will be addressed in Chapter 3.

2.3 Overview of Reverse Electrodialysis

The main competing technology for salinity gradient power generation is reverse

electrodialysis (RED). In contrast to the PRO system, which uses water-permeable membranes,

the RED system uses ion-selective membranes, with the electrical current associated with the

movement of the positive and negative ions providing a direct source of electricity without the

need for a turbine. The mirror image of RED is the process of electrodialysis, which uses

electricity and ion-selective membranes for desalination. In contrast, RED directly produces

electricity from the chemical potential energy through the controlled mixing of seawater and

fresh water, operating like a "salinity battery" [26].

To harness the energy of the salinity gradient in this manner, a RED stack is used. In this

setup, compartments are created by alternating cation-exchange membranes (CEM, which are

selectively permeable to positive cations like Na^+) and anion-exchange membranes (AEM,

permeable to anions like Cl⁻). Fresh water and seawater flow through the compartments between

the membranes in an alternating pattern.
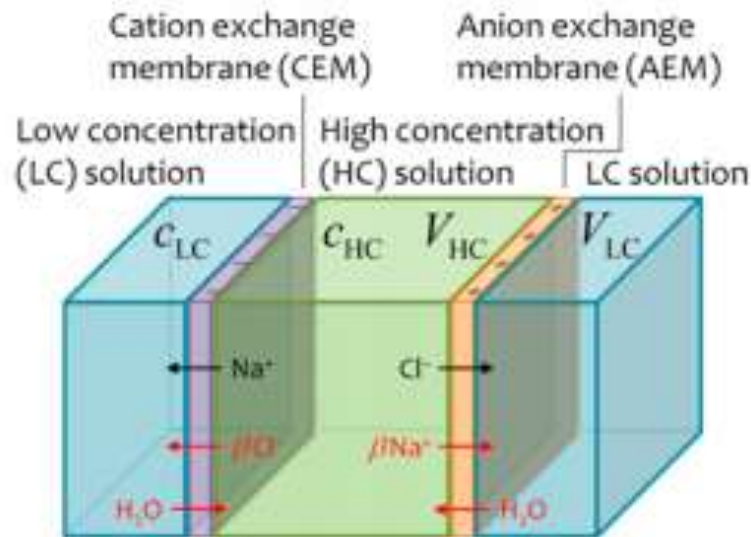
Figure 6 is a diagram of one RED cell within the stack, consisting of one high-

concentration solution compartment and two low-concentration half-compartments. Because of

the chemical potential difference between the solutions, cations from the high-concentration

solution pass through the CEM, which has a fixed negative charge, while anions pass through the

AEM, which has a fixed positive charge. The salinity gradient causes a potential difference of

80-100 mV to form across each membrane, which is known as the Nernst potential or the

membrane potential [20]. By repeating this cell configuration many times to form a stack, a

significant overall potential difference can be created – the sum of the potential differences over

each membrane. A cathode and an anode are placed at the ends of the stack and maintain

electro-neutrality of the solutions in the electrode compartments through redox reactions. In this

way, electrons can be transferred from the anode to the cathode via an external electric circuit.

The potential difference and current flow between the electrodes results in electrical power when

an external load is included in the circuit.
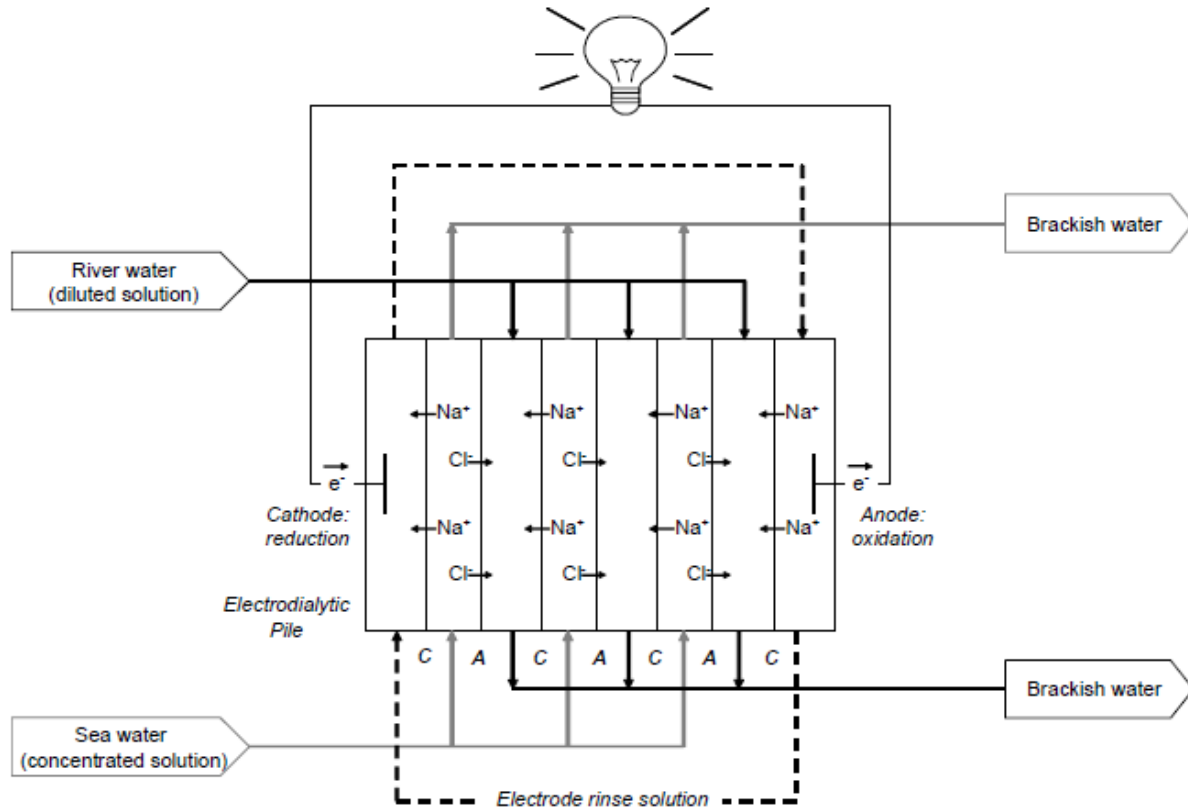
Figure 7: Diagram of a RED system with N=3 cells [20]

In contrast to PRO, which uses a membrane module and turbine generator, the RED

process is able to directly produce electricity in one step. Despite this advantage, there are

several inherent limitations to the RED process. The most serious technical limitation to power

generation through RED is the inherent electrical resistance provided by the RED stack. In the

ideal case, the RED stack would have no internal resistance so that the sum of the membrane

potential differences would be equal to the output voltage from the RED stack. In reality, however, the membranes and the solutions in the stack have significant electrical resistance, which combine to determine the overall resistance of the RED stack. In most cases, the majority of the resistance is due to the resistance of the ion exchange membranes. Typical literature values for ion exchange membrane area-specific resistance range between $0.7 - 11$ Ω cm^2 [26].

The resistance of the solutions that are pumped through the chambers in the RED stack also contributes to the overall stack resistance. This is especially important at the beginning of the RED process because there is very little salt in the compartments containing the low concentration solutions, causing the resistance of these solutions to be very high. As salt permeates from the high concentration solution to the low concentration solution, this resistance decreases significantly. For NaCl solutions, the molar conductivity is approximately 0.09 mS cm^{-1} mM^{-1} for solutions less than 1 M in concentration [26]. Typical inter-membrane distances in the literature range from 60-500 μm, with the most common being 150 μm [26]. Based on this, seawater (600 mM NaCl) has an area-specific resistance of 0.28 Ω cm^2 and brackish water (17 mM NaCl) has an area-specific resistance of 9.8 Ω cm^2.

The output voltage from the stack is equal to the ideal voltage minus the voltage drop across the stack. The voltage drop across the stack depends on the relative values of the stack resistance and the load resistance—the higher the ratio of the load resistance to the stack resistance, the lower the current through the circuit and the closer the system approaches ideality. However, very high resistance also means that there will be very low current output. The time required for the RED process to proceed is proportional to the current that is generated from the process [26]. From a practical standpoint, there is a trade-off between the amount of energy that

is wasted due to internal resistance and the time required for the energy to be generated. Even when membrane power density is maximized, approximately 55% of the available mixing energy is lost to internal resistive dissipation alone [26]. A further 20% of the available mixing energy is lost due to imperfect membrane selectivity, i.e. co-ion leakage across the ion exchange membranes [26].

Higher energy recovery efficiencies are needed to make the technology viable, which requires research in techniques to reduce the RED stack resistance. Currently, power densities in the range of $0.4 – 1.2$ W/m^2 have been reported, which must be increased to at least 5 W/m^2 in order for the technology to be feasible [20]. On the other hand, PRO power densities exceeding 10 W/m^2 have been reported [27].

In addition to the technical challenges, the economics of RED present obstacles to implementing the technology on a large scale in the near future. The greatest obstacle is current membrane prices. Because ion exchange membranes currently serve a very small and specialized market segment, membrane prices can exceed \$100/m^2 [20]. In order to be competitive, the price needs to decrease by at least two orders of magnitude. Currently, the cost of PRO membranes is on the order of \$30/ m^2, and the prospect for further cost reduction is possible as water desalination using reverse osmosis (RO) becomes more prevalent since both RO and PRO employ similar membranes.

As a result of the technical and economic challenges facing RED at this point, it was decided to focus the remainder of this analysis on PRO as it currently appears to be a more likely candidate for a feasible energy generation technology in the Gambia.

2.4 Current Technology Status

In November 2009, Statkraft began testing osmotic power production at a 10 kW PRO pilot plant in Tofte, Norway [28]. The facility was designed to evaluate membrane performance, optimize operating conditions, test pressure exchanger operation (recovery of energy from the low pressure brackish water), and research pretreatment requirements for both the fresh water and seawater streams [29]. The facility used approximately 2000 m^2 of membranes during operation— from 2009-2011, the membranes were spiral wound cellulose acetate membranes and from 2011 onwards the membranes were spiral wound thin film composite (TFC) polyamide membranes [29]. In December 2013, Statkraft announced that it would be discontinuing investment in osmotic power technology based on current market conditions to focus on "more competitive and relevant investments" [30]. In November 2014, the Dutch king inaugurated the first RED power plant located on the Afsluitdijk in the Netherlands [31]. The 50 kW pilot plant will conduct experiments on reverse electrodialysis power generation.

Besides these pilot plant facilities, research on PRO and RED is being conducted in a large number of major universities around the world. Current areas of research are generally focused on membrane characteristics and process optimization. Membrane research includes fabrication of membranes with higher permeability and selectivity, as well as work to minimize concentration polarization and membrane fouling [24]. Process optimization includes research on the best operating conditions for PRO and improving RED stack design [20, 25].

Chapter 3

Practical Limitations of Salinity Gradient Power Plants

Salinity gradient power has been studied since the mid-1950s, but most of the literature has been focused on theoretical analyses or bench-scale experiments [20]. Pilot plants to test the viability of a full-scale implementation are a very recent phenomenon that has occurred only in the last five years. According to Yip et al., the theoretically available energy from reversibly mixing fresh water (~0.01 M NaCl) in an infinite reservoir of seawater (~0.5 M NaCl) is 2.76 MJ/m^3 of fresh water [21]. However, PRO is an irreversible process which generates entropy. As a result, the amount of useful work that can be extracted from the salinity gradient is limited by inefficiencies in the actual process, which depend on the specifics of the system design and operation.

In addition, the optimal design of a salinity gradient power plant must account for the overall economics of energy production, which are typically dominated by the cost of the membranes. Thus, a large portion of the literature has focused on the energy density of the particular process (in W/m^2 of membrane area), which is distinct from the energy recovery efficiency (energy recovered relative to the theoretical maximum). The process conditions which maximize the power density are not the same as the process conditions which maximize the energy recovery from the mixing of the streams. In practical applications, these two goals directly compete with each other: as energy recovery increases, power density decreases.

The design and operation of a Gambian salinity gradient power plant must strike a careful balance between these two objectives, with the goal of achieving as much usable power for the

population as possible but at an appropriate cost. The overall economic viability of a salinity

gradient power plant will depend on the efficiency of the energy extraction technology, the

capital and operating costs of the plant, and the sale price of the energy that is produced. The

purpose of this chapter is to explore the first of these considerations: the efficiency of PRO

technology for energy extraction. Practical limitations of the technology will be analyzed in

order to provide a best estimate for energy recovery efficiencies and power densities.

3.1 Effect of Mixing Proportion and Non-ideal Solution Behavior

Before considering the energy recovery efficiency, it is necessary to revisit the

assumptions used to calculate the theoretical amount of energy released from the salinity

gradient. Because the energy released by mixing increases as the entropy of the mixture

increases, the fresh water was assumed to be mixed with an infinite quantity of salt water in the

original calculation. This assumption was made so that entropy would be maximized in the

brackish water outlet, which occurs when the salt concentration of the brackish water is

essentially equal to the salt concentration of the seawater inlet. However, in a real system, the

salt concentration of the brackish water outlet will be somewhat less than the concentration of

the seawater – the use of an "infinite" volume of seawater would require unacceptably large

pumps for the initial pressurization, making the overall process economically infeasible.

Therefore, the energy of mixing in any real systems not only depends on the salt concentrations

of the feed solutions, but also on the ratio of fresh water feed (N_A) to seawater feed (N_B), as

shown in Figure 8 [21].
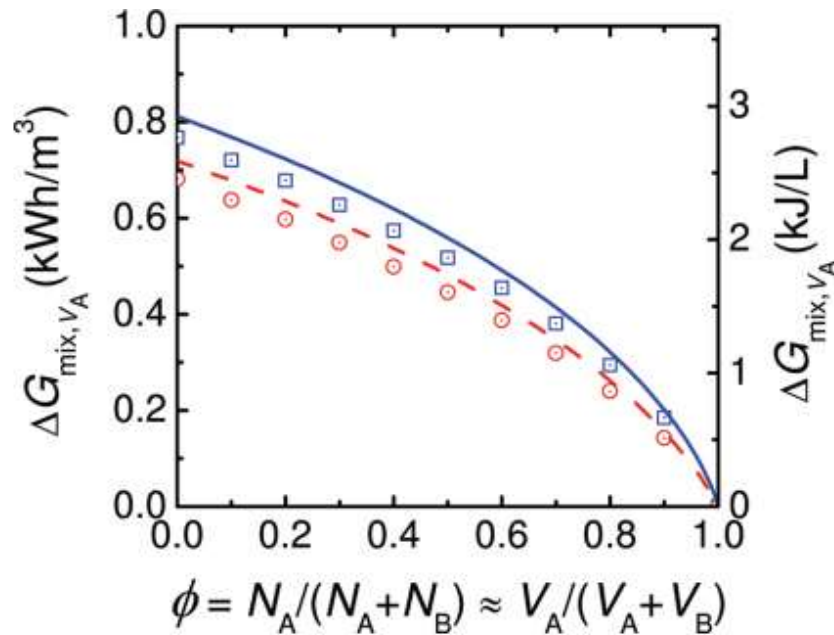
Figure 8: Gibbs free energy of mixing as a function of mixing ratio [21]

Although more energy is released as the seawater ratio increases ($\phi \rightarrow 0$), energy is required to pump the seawater into the power plant. As a result, there is a point of diminishing marginal return; this determines the optimal feed ratio based on the pumping cost of the seawater source. Fortunately, as the Gambia is a very flat country, there will be little cost associated with raising the water above sea level. Instead, the pumping cost will be dominated by overcoming friction losses due to viscous effects in the piping (in addition to the capital cost of the pumps). Typically, literature studies use feed ratios between 0.4 and 0.5 as a base case assumption, resulting in a Gibbs free energy of mixing between 2.0-2.2 MJ/m³ for a fresh water (1.5 mM) feed solution and 1.7-1.9 MJ/m³ for a brackish water (17 mM) feed solution [21].

In Chapter 2, the equations derived for PRO assumed ideal solution behavior; that is, the activity coefficients for the solutions were assumed to be 1 so that the entropy of mixing is

directly related to the logarithm of the mole fractions (Equation 3). In reality, the activity

coefficients are typically less than 1 for the solution concentrations of interest due to interactions

between the ions and with the water. These effects are shown in Figure 8, which is based on

modeling done by Yip et al. [21]. The solid blue and dashed red curves represent values for ideal

solutions while the symbols represent values calculated using the measured activity coefficients

of the different salt solutions. The solid blue curve and square symbols represent mixing river

water (1.5 mM or 88 mg/L NaCl) with seawater (600 mM or 35 g/L NaCl) at 298 K. The dashed

red curve and open circles represent mixing brackish water (17 mM or 1000 mg/L NaCl) with

seawater at 298 K. For these calculations, the mole fraction of fresh water or brackish water is

approximately equal to the volumetric fraction because the solution concentrations are dilute.

Inclusion of the activity coefficients in the modeling gives a calculated energy of mixing that is

5 - 9% less than the energy predicted assuming ideal solution behavior, or approximately 1.8-2.0

MJ/m^3 for a fresh water (1.5 mM) feed solution and 1.6-1.8 MJ/m^3 for a brackish water (17 mM)

feed solution [21].

3.2 Inherent Constraints of PRO

In order to achieve 100% recovery of the Gibbs free energy of mixing, a reversible work

extraction process is required. This is theoretically possible for the PRO process and has been

described by Yip et al. [21]. Essentially, this process consists of applying a hydraulic pressure to

the draw stream that is negligibly smaller than the osmotic pressure difference so that an

infinitesimally small volume of water passes through the membrane. As this process occurs, the

saline solution is diluted and the osmotic pressure difference is reduced. The hydraulic pressure

is simultaneously reduced to allow another infinitesimal volume of water to permeate. This

process is continued until the osmotic pressure difference is zero and the water flux stops.

Although this reversible work extraction process could theoretically recover 100% of the Gibbs

free energy of mixing, the membrane area that would be required approaches infinity in order for

the process to run in a finite time period. As a result, the power density of the process would

approach zero, making it economically impractical.

In comparison, an actual PRO process typically operates at a constant draw pressure

which is less than the osmotic pressure difference. This simplifies the design to better suit

available membrane technology, equipment, and control schemes. In this case, the maximum

amount of extractable work is limited by frictional losses and underutilized energy, as shown in

Figure 9.
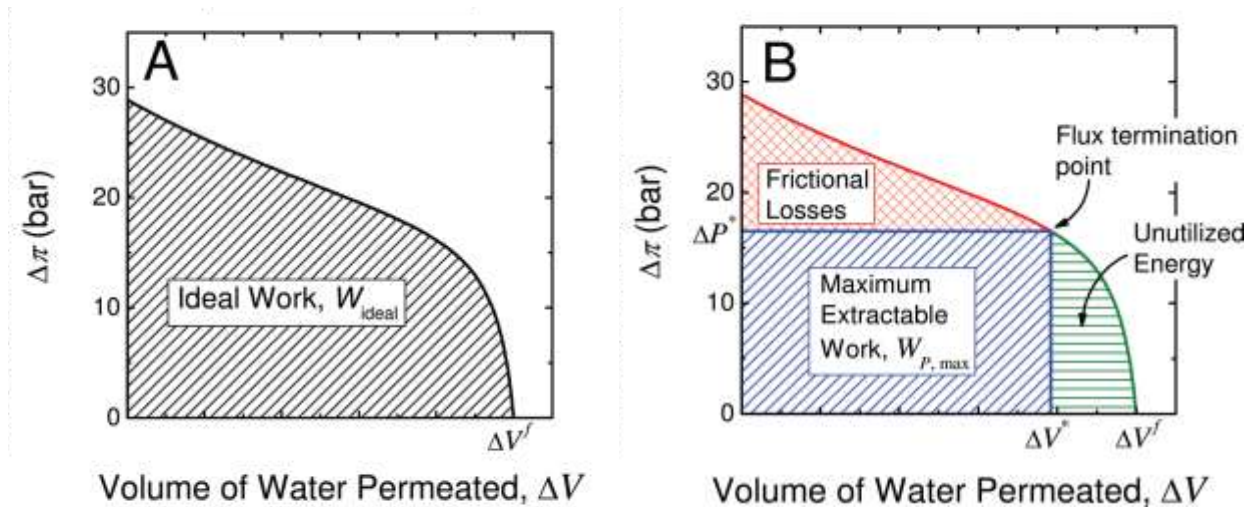
Figure 9: Comparison of: (A) reversible and (B) constant-pressure PRO operation for mixing seawater and brackish water with feed ratio = 0.4 [21]

Initially, the osmotic pressure driving force is significantly greater than the applied draw pressure, resulting in a large driving force for water flux across the membrane. Because the final pressure is set by the draw pressure, the excess energy is lost in the form of friction losses due to the hydraulic resistance of the membrane (the inverse of the permeability) as the water flows from the low salinity stream to the high salinity stream [21].

The second type of loss, unutilized energy, arises because the constant applied draw pressure limits the membrane permeate volume. Instead of continuing until the osmotic pressure difference is zero, the water flux stops when the osmotic pressure difference is equal to the applied draw pressure. The energy recovery efficiency is defined as the maximum extractable work divided by the Gibbs free energy of mixing. Energy recovery efficiency of constant-pressure operation is a function of both feed and draw solution concentrations and the feed ratio. Energy recovery and efficiency for mixing seawater and brackish water as a function of feed ratio is shown in Figure 10.
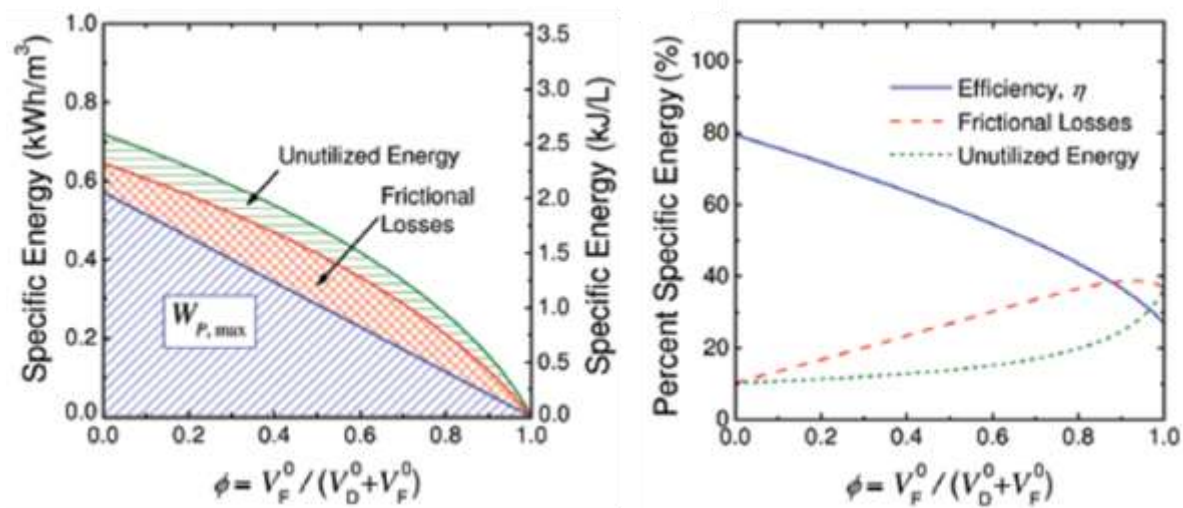
Figure 10: Energy recovery efficiency of constant-pressure PRO for mixing seawater and brackish water [21]

A summary of the approximate energy recovery, efficiency, and losses for typical feed ratios is shown in Table 3.

Table 3. Recovery and efficiency for feed ratios of 0.4 and 0.5 [21]

	Fresh Feed (1.5 mM)		Brackish Feed (17 mM)	
Feed Ratio	0.4	0.5	0.4	0.5
Energy Recovery (MJ/m^3)	1.6	1.3	1.2	1.0
Recovery Efficiency	72 %	67 %	63 %	60 %
Frictional Losses	23 %	28 %	24 %	26 %
Unutilized Energy	5 %	5 %	13 %	14 %

The power density of the PRO system is directly proportional to the water flux and the draw pressure. In turn, the water flux is proportional to the membrane permeability and the difference between the osmotic driving force and the draw pressure. As mentioned previously, the power density decreases with increased permeate volume. In actual operation, the power density requirement for economic operation will limit the permeate volume to less than the maximum possible volume for a given draw pressure. In this case, the optimum applied draw pressure will shift downwards to maintain membrane flux. As a result, the optimal operating pressure will be determined by the extent of water permeation across the membrane.

All other things being equal, a higher membrane permeability equals higher water flux and therefore higher power density, which moves the permeate volume limit closer to the maximum for a given draw pressure. However, membrane selectivity is also a consideration as no membrane is able to perfectly reject all salt ions in a solution. Increased water permeability typically comes at the price of decreased membrane selectivity – this tradeoff between permeability and selectivity is inherent to all membrane processes. As more salt is able to pass through the membrane, the water flux decreases due to the reduction in the osmotic pressure difference, which provides the driving force for water transport. Therefore, increased membrane permeability has to be balanced against the corresponding reduction in salt retention.

In order to withstand the mechanical stress resulting from operating pressures on the order of 10 bar, PRO membranes must have a support layer(s) to increase the overall strength of the membrane. However, these internal support layers give rise to internal concentration polarization (ICP). ICP occurs due to permeation of the salt into the porous support layer, causing the salt concentration difference across the active layer of the membrane (the driving force for the osmotic flow) to be less than the difference in salt concentration between the fresh water and seawater solutions as shown in Figure 11. The effects of ICP can be minimized by reducing the thickness of the support layers, although this can compromise the overall mechanical integrity of the membrane thereby limiting the range of feasible PRO operating pressures.
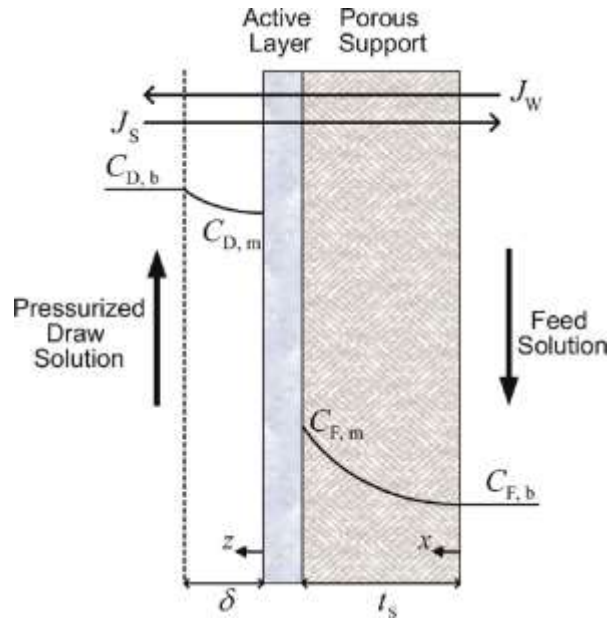
Figure 11: Schematic of the steady-state salt concentration profile [27]

Membranes designed for PRO plants have to balance the trade-offs between membrane permeability and selectivity as well as the tradeoff between ICP and PRO operating pressure (arising from the membrane support layers). Membrane life and cost will also play a critical role in the overall economic feasibility of a PRO plant. The effects of these parameters are investigated in more detail in the following chapter.

Chapter 4

Economic Analysis of PRO Installation

A high-level economic analysis of the production of electrical power using pressure retarded osmosis (PRO) was conducted to understand the short-term and long-term viability of the process in the Gambia. Model inputs include feed and draw solution concentrations, membrane characteristics, plant operating conditions, and estimates for plant capital and operating costs. Based on these input values, the model evaluates the water flux, power density, plant size, plant capacity, and efficiency. To compare PRO to other possible sources of electricity, the model was also used to evaluate the break-even price of electricity generation using PRO.

The main cost driver for the energy produced at a PRO plant is the membranes, which can account for over 80% of plant cost year-to-year. As the PRO technology is still very new, development of membranes with improved performance or lower cost is possible as the technology matures. The five key variables determining the total annual cost of the membranes at the PRO plant are the membrane permeability (a measure of water flux), the selectivity (a measure of salt retention), structural parameter (a measure of internal concentration polarization), membrane life, and material price per unit area. Therefore, a sensitivity analysis was conducted on these five key variables to identify the importance of these parameters on the overall cost, as well as to determine the effects of different technological advancements on the economics of the PRO process.

4.1 Methodology and Assumptions

In Chapter 2, Equation (6) was used to calculate the permeate volume as a function of the

membrane water permeability coefficient k_p, membrane area A, osmotic pressure difference $\Delta\pi$,

and operating pressure difference ΔP. This equation can be rearranged to evaluate the water flux

J, defined as the volumetric water flow rate per unit membrane area.

$$J = k_p \, (\Delta\pi - \Delta P)$$ [9]

However, Equation (9) assumes that there is no salt transport across the membrane and neglects

the effects of internal concentration polarization as described in Chapter 3. These phenomena

were included in the PRO model using the modified flux equation derived by Yip et al. [27]

based on solution of the mass balances and mass transfer equations for the water and solute:

$$J = k_p \left(\frac{\pi_D \exp\left(-\frac{J}{k_c}\right) - \pi_F \exp\left(\frac{JS}{D}\right)}{1 + \frac{k_s}{J}\left(\exp\left(\frac{JS}{D}\right) - \exp\left(-\frac{J}{k_c}\right)\right)} - \Delta P \right)$$ [10]

In this expression, π_D is the bulk osmotic pressure of the draw solution, π_F is the bulk osmotic

pressure of the feed solution, k_c is the solute mass transfer coefficient in the bulk solution, D is

the solute diffusion coefficient, k_s is the membrane solute permeability coefficient, and S is the

membrane structural parameter. Note that Equations (9) and (10) both assume that the osmotic

reflection coefficient of the membrane is equal to one, which is only rigorously true for a

membrane that is completely retentive to salt. The power density is simply the product of the

membrane flux and the operating pressure:

$$PD = J * \Delta P$$ [11]

In this analysis, the solute was assumed to be pure NaCl, which has a diffusion

coefficient $D = 1.99 * 10^{-9}$ m^2/s [27]. The bulk mass transfer coefficient is a function of the

solute (salt) diffusion coefficient, the feed flow rate, and the module design, e.g., the properties

of the spacer used in the spiral wound module. Values in the literature range from approximately

20 μm/s to 60 μm/s; all calculations in this thesis were performed using $k_c = 38.5$ μm/s [27].

Although sodium chloride makes up about 85-90% of the salt content of actual seawater, there

are also significant amounts of sulfate, magnesium, calcium, and potassium ions [32]. The

presence of these ions should not change the calculated values of the water flux by more than

10%, especially because most of these ions are larger than Na^+ and Cl^- and would thus be more

effectively rejected by the PRO membrane.

Based on the Morse equation from Chapter 2, the osmotic pressure of an ideal solution is

linearly proportional to the solute concentration. In order to calculate the bulk osmotic pressure

of the feed and draw solutions, a correlation was created using osmotic pressure data from Yip et

al. at a temperature of 298 K [27].
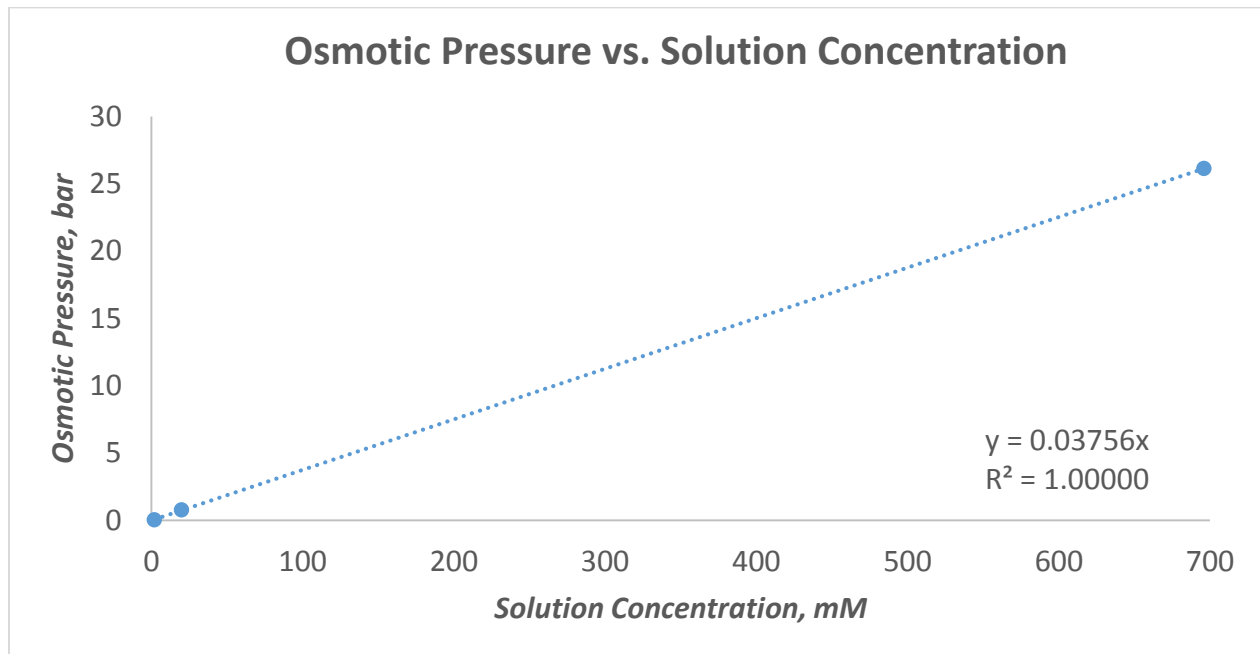
Figure 12: Correlation to determine osmotic pressure as a function of concentration

Based on this correlation, the van't Hoff factor for sodium chloride is 1.52. The bulk osmotic

pressure was calculated using Equation (12), which is equivalent to the Morse equation

(Equation 4) at 298 K using more convenient units for pressure and concentration. Deviations

from ideal behavior at higher salt concentrations were not included in the analysis.

$$\pi = 0.03756 \frac{bar}{mM} * c \qquad [12]$$

In the PRO installation, it was assumed that the fresh water feed was mixed with an equal

volume of seawater draw solution (i.e., the inlet volumetric flow rates of the fresh water and

seawater were assumed to be equal), giving an overall feed ratio of 0.5. As water and salt

permeate across the membrane, the concentrations of the feed and draw solutions will change.

The permeate fraction, δ, is defined as

$$\delta = \frac{\Delta V}{Q} \qquad [13]$$

where ΔV is the volumetric permeate flow rate and Q is the inlet volumetric flow rate of the fresh

water feed. For this analysis, the flow rate of the fresh water feed was assumed to be 10 m^3/s,

which is 50% of the approximate projected baseline flow rate of the Gambia River after the

completion of the Sambangalou Dam in 2018 [33]. This provides an estimate of the maximum

possible energy generation from a PRO system on the Gambia River – higher fresh water flow

rates would not be sustainable. The permeate fraction can be controlled by the design of the

membrane module, the feed flow rate, and the operating pressure of the system. Larger

membrane modules or lower flow rates provide longer residence times and thus larger permeate

fractions. A lower operating pressure yields a larger permeate fraction by increasing the driving

force for water transport across the membrane (greater difference between the osmotic and draw

pressures).

The concentrations of the feed and draw solutions inside the membrane module can be

calculated as a function of the permeate fraction as given by Equations (14) and (15).

$$c_f = \frac{c_{f,0}}{1 - \delta} \qquad\qquad [14]$$

$$c_d = \frac{c_{d,0}}{1 + \delta} \qquad\qquad [15]$$

The use of Equations (14) and (15) assumes that the PRO membranes are sufficiently selective

that the concentration of the solutions is dominated by the extent of water transport, with

negligible contribution due to salt transport. In reality, salt transport will cause a small increase

in the salt concentration in the fresh water stream, with the reverse for the draw (seawater),

further reducing the energy generation from PRO.

As water permeates across the membrane, the variation in salt concentrations also

reduces the osmotic pressure difference. Figure 13 shows a plot of the osmotic pressure

difference and water flux as a function of the permeate fraction using reasonable estimates for

the membrane properties.
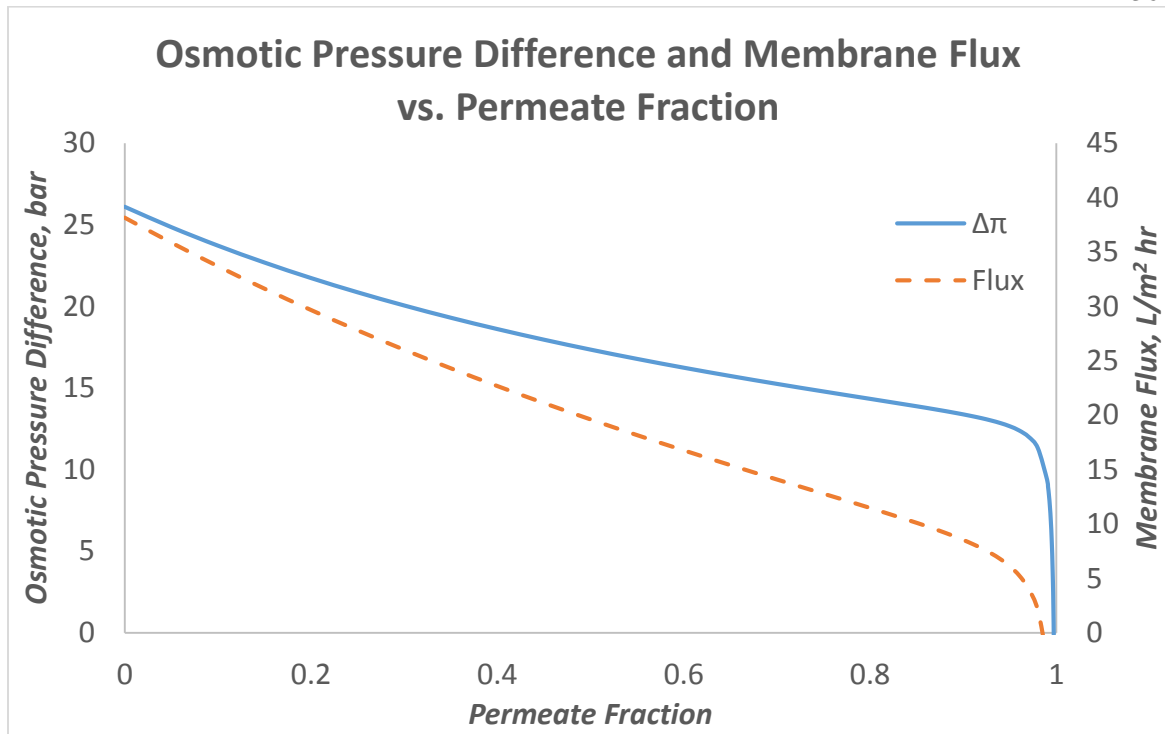
Figure 13: System behavior as a function of permeate fraction
$c_{f,0} = 1$ mM, $c_{d,0} = 696$ mM, $k_p = 5$ L/m² hr bar, $k_s = 1$ L/m² hr, $S = 307$ µm, $\Delta P = 10$ bar

Because the salt concentration in the fresh water feed is very low, the change in the osmotic pressure difference is dominated by dilution of the more concentrated draw solution until one gets to very high permeate fractions. The net result is that the osmotic pressure difference and the water flux vary approximately linearly with the permeate fraction for $\delta = 0$ - 0.9. Significant differences from this linear relationship are only seen at very high permeate fractions due to the significant increase in the salt concentration of the feed solution under these conditions.

The membrane area required for the PRO plant was calculated based on the permeate volume and the average membrane flux. The average water flux was evaluated as:

$$J_{avg} = \frac{\int_0^V J(V)dV}{V} \approx \frac{J_{initial} + J_{final}(\delta)}{2} \quad for \ 0 \le \delta < 0.8 \qquad [16]$$

based on the linear relationship between the flux and the permeate fraction seen in Figure 13.

Therefore, the membrane area can be calculated as

$$A = \frac{\Delta V}{J_{avg}} \approx \frac{2 \delta Q}{J_{initial} + J_{final}(\delta)} \quad for \ 0 \le \delta < 0.8 \qquad [17]$$

The efficiency of energy extraction of the membrane system is equal to the amount of

work extracted from the mixing process divided by the theoretical (ideal) change in the Gibbs

free energy due to mixing. Based on the discussion in Chapter 3, the total available energy of

mixing equal volumes of fresh water and seawater is 1.3 MJ/m^3, and the inherent frictional losses

and underutilized energy from the PRO system limit the recovery efficiency to a theoretical

maximum of 67% of this value [21]. The recovery efficiency of an actual system was assumed

to be approximately linearly proportional to the permeate fraction; that is, the larger the permeate

fraction, the closer the recovery efficiency comes to the theoretical maximum. Parasitic losses

from friction in the piping and membrane modules as well as inefficiencies in the rotating

equipment further limit the system efficiency. In this analysis, approximately 10% of the

available energy was assumed to be consumed by these parasitic losses, giving a rotating

equipment efficiency of $\eta_{RE} = 90\%$. This assumption is optimistic but can be reasonably

achieved if energy recovery devices such as pressure exchangers are used to pressurize a portion

of the incoming draw solution using the residual pressure from the brackish water exit.

Therefore, the overall system efficiency was calculated as follows:

$$\eta_{actual} = \eta_{max} * \eta_{RE} * \delta = 0.67 * 0.9 * \delta \qquad [18]$$

From this, the plant power output can be calculated based on the permeate volume. It is assumed that the plant is fully online 95% of the year, with planned and unplanned maintenance making up the balance of time.

$$Capacity\ (MW) = 0.95 * \eta_{actual} * \delta * Q * \Delta G_{mix} \qquad [19]$$

The optimal operating pressure is also found to be a function of the permeate fraction, which balances the effects of the operating pressure on water flux and power production. Given a value for the permeate fraction, the optimal operating pressure is the point at which the average power density is maximized. The results of this analysis are shown in Figure 14 and Table 4.
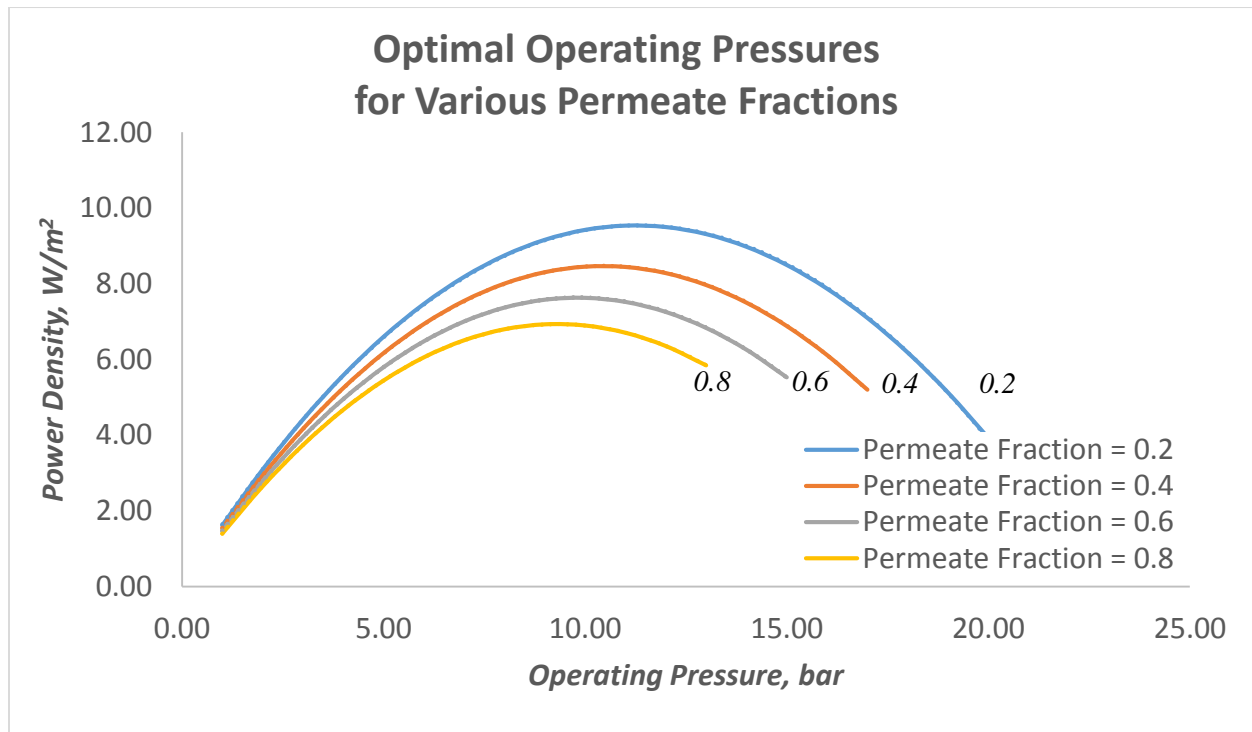
Figure 14: Determination of optimal operating pressure as a function of δ
$c_{f,0}$ = 1 mM, $c_{d,0}$ = 696 mM, k_p = 5 L/m² hr bar, k_s = 1 L/m² hr, S = 307 μm

The average power density decreases with increasing permeate fraction, although operating at high permeate fractions does lead to a higher efficiency and energy recovery. As the permeate fraction increases, the optimal operating pressure decreases to allow higher membrane flux as seen in Table 4.

Table 4. Optimal operating pressure for various values of permeate fraction

Permeate Fraction	Optimal ΔP (bar)
0.2	11.30
0.4	10.47
0.6	9.83
0.8	9.31

To conduct the sensitivity analysis, the values of membrane permeability, selectivity, structural parameter, membrane lifetime, and membrane price per unit area were varied for each of several values of the permeate fraction using the corresponding optimal pressure.

4.2 Cost Methodology and Assumptions

The total cost of a PRO plant consists of the capital and operating expenses. The capital expenses include all of the one-time, up-front costs associated with designing and building the plant. These expenses include:

- Civil and structural costs associated with site preparation and construction of buildings

- Purchase and installation of major mechanical equipment

- Purchase and installation of electrical instrumentation and control (I&C) equipment

- Construction labor and management

- Engineering design fees

- Feasibility, development, and environmental studies

- Legal fees and permitting

- Taxes

- Contingency costs

Operating expenses include all of the day-to-day, ongoing costs associated with running the PRO plant. These can include:

- Membrane cleaning costs

- Membrane replacement costs

- Cleaning chemicals, lubricants, and other supplies

- Minor maintenance, repairs, and spare parts

- Major equipment overhauls

- Labor costs for plant operation

- General and administrative expenses

- Insurance

- Taxes

As PRO is still a developing technology, the costs of a pioneer plant will be much larger than for an nth-generation plant design due to the risks of less-than-anticipated plant performance

and capital budget underestimation. These risks and the costs associated with design and installation of these plants decrease over time as equipment manufacturers, plant owners, and construction companies gain experience with the technology. For this analysis, it was assumed that a PRO installation in the Gambia would be an nth-generation plant rather than one of the early versions of a PRO plant.

The U.S. Energy Information Administration (EIA) conducted a 2013 study on the capital costs of utility-scale electricity generation plants. Coal, natural gas, nuclear, biomass, wind, solar, geothermal, and hydroelectric power generation technologies were analyzed in twenty-six different case studies. For each case, capital and operating expense estimates for a generic U.S. power plant were presented based on industry data and experience from the consulting firm SAIC. Capital cost data was given for each of the technologies in the following categories: Civil/Structural, Mechanical Equipment, Electrical Equipment, Project Cost (e.g., engineering design, construction labor and management, and commissioning cost), Owner Cost (e.g., preliminary studies, property cost, legal fees, permitting, and insurance), and Contingency. Additionally, estimates were given for the operating costs of the different processes.

The only PRO pilot plant in the world was built by Statkraft in Norway, and specific cost and operation data for that plant are not publicly available; there are currently no full-scale PRO installations. Therefore, the EIA capital cost data were used to perform a high-level cost analysis for a PRO plant. First, of the 26 different cases in the EIA report, 21 were chosen as most applicable for this analysis. Data were not considered for a dual unit uranium nuclear power facility (due to the extremely high capital costs associated with this facility) as well as cases involving coal and natural gas combustion employing advanced carbon capture and storage technology (because PRO involves no carbon emissions). Next, the cost data was normalized on

a per-megawatt basis (for facilities with capacities ranging from 20 MW to 1300 MW). Cost

averages were then developed to estimate average costs for all technologies; a separate average

was determined based on data for the renewable technologies (e.g., geothermal, hydroelectric,

wind, solar).

Table 5. Capital cost estimates, determined from data in EIA report [34]

Cost Type	All Cases		Renewables	
Capital Costs	**($MM/MW)**	**% of total**	**($MM/MW)**	**% of total**
Civil/Structural	0.50	12%	0.74	16%
Mechanical Equipment	1.83	44%	2.29	44%
Electrical I & C	0.31	8%	0.37	8%
Project Costs	0.50	13%	0.54	10%
Owner Costs	0.61	15%	0.71	13%
Contingency	0.35	8%	0.43	8%
TOTAL CAPEX	*4.10*	*100%*	*5.07*	*100%*
Operating Costs	**($MM/yr/MW)**	**% of total**	**($MM/yr/MW)**	**% of total**
TOTAL OPEX	*0.13*	*100%*	*0.12*	*100%*

For all capital expense categories, the cost estimates were higher for the renewable

technologies, but the general cost breakdown was similar (Figure 15). The cost of mechanical

equipment makes up almost half of the project cost for most of the cases, with each of the other

categories comprising about 10-15% of the total costs. The cost premium for renewable projects

is 47% for civil and structural costs, about 20-25% for mechanical and electrical equipment, and

about 10-15% for project and owner costs. Since the renewable technologies would seem to be

more representative of a PRO plant, these values were used to calculate the civil/structural,

electrical I&C, project cost, owner cost, contingency, and operating costs of the PRO plant in the

model. Additional contingency was considered but ultimately not included due to the

assumption of an nth-generation plant employing mature technology.
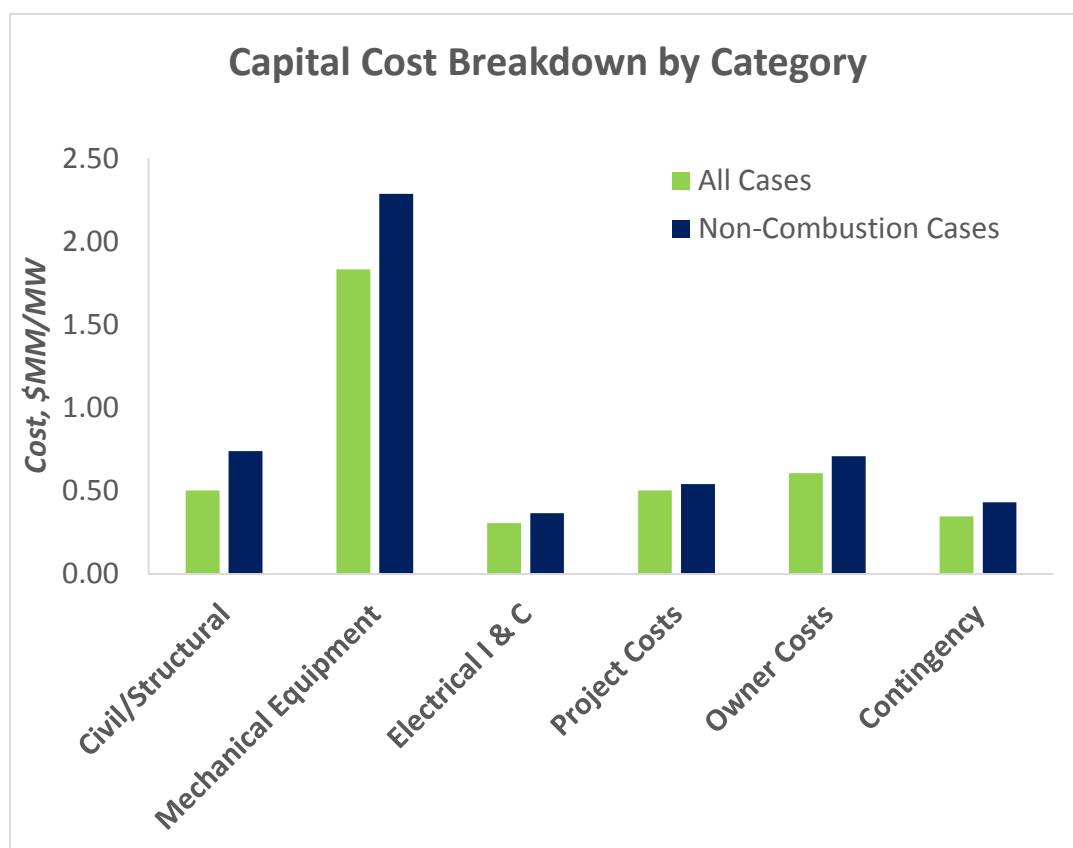
Figure 15: Average capital cost by category, adapted from EIA report [34]

Because the cost of mechanical equipment was such a large part of the total project

capital cost, it was desirable to have a more accurate estimate for this contribution. First, it was

assumed that the equipment costs would be dominated by the membrane cost and the cost of the

turbine and pumps. The membrane cost was calculated based on the membrane area, membrane

price per unit area, and membrane lifetime. It was assumed that the membranes would be replaced on a rotating schedule in the plant and that the cost of membrane replacement could be spread evenly over time. Base case assumptions for membrane cost (C_{mem}) and life (L_{mem}) are $30/m^2 and 3 years based on characteristics of currently available RO membranes [35]:

$$Membrane\ Cost = \frac{A * C_{mem}}{L_{mem}} \qquad [20]$$

There are three main types of hydraulic turbines: Pelton, Kaplan, and Francis. Pelton turbines are typically used in high head, low flow applications. Conversely, Kaplan turbines are most common in low head, high flow rate applications. Francis turbines are a hybrid style which can accommodate a medium range of flow rate and head conditions; these are the most likely candidate for use in a PRO plant. The following equation was used to estimate the cost of a Francis turbine as a function of the operating conditions, valid for flow rates in units of m^3/s and pressure in units of bar [36]:

$$Turbine\ Cost\ (\$) = 451,200 * \left(\Delta V * \sqrt{10.2 * \Delta P} \right)^{0.11} \qquad [21]$$

The total cost of all mechanical equipment (including pumps) was simply estimated as twice the turbine cost:

$$Mech.\ Equip.\ Cost\ (\$) = 2 * Turbine\ Cost\ (\$) \qquad [22]$$

Financing is a key part of any project of this scale. Generally, loans are used to pay for the capital costs of the project with associated agreements about interest rates and payment schedules. Often, these agreements can determine the financial success or failure of a given venture and need to be carefully considered prior to moving forward with a detailed analysis. The cash flow projections, depreciation, interest calculations, and other financial considerations for a project of this scale and complexity were beyond the scope of this study. Instead, the

payment schedule for the capital costs was assumed to be evenly spread over the projected 30-

year life of the plant.

As discussed previously, the Gambian government passed the Renewable Energy Act in

2013, which exempts renewable energy projects from import, corporate, and value-added taxes

for fifteen years from commissioning [15]. Additionally, the European Union has expressed

willingness to provide financial support for development of renewable energy projects in the

Gambia. Therefore, no taxes or interest were included in calculating the capital costs of the PRO

plant. However, no further government subsidies were included for the power produced from the

plant to provide a direct comparison to other energy generation technologies.

To verify the validity of the assumptions that were made, model calculations were

compared with published data for the performance of the Statkraft pilot plant. In an analyst

report, Statkraft executives stated that their PRO plant would be competitive if a power density

of 5 W/m^2 could be achieved [37]. The revenues for a power plant are based on the plant power

generation capacity and the price of electricity. The costs of the plant are based on the cost of

the membrane material, the membrane lifetime, and the amortized non-membrane costs. Based

on these revenue and cost data, the minimum average power density for the plant to break even

financially can be calculated as:

$$PD_{avg} = \frac{\left(\frac{C_{mem}}{L_{mem} * C_{power}}\right)}{\left(1 - \frac{C_{other}}{C_{power} * Capacity}\right)} \qquad [23]$$

For a 3 MW PRO plant using a membrane cost of \$30/m^2, a membrane life of 3 years, an energy

price (C_{power}) of \$0.26/kWh, and other (non-membrane) costs (C_{other}) of \$650,000/yr, the average

power density given by Equation (23) was 4.9 W/m^2, which is in excellent agreement with

published analyses. This suggests that the cost assumptions made in the current analysis provide

a reasonable framework for evaluating the overall economics of a PRO facility.

The most effective way to judge the economic viability of a potential energy production

technology is the cost of the energy produced. For the PRO plant, the cost of power that is

required to break even financially can be calculated as follows:

$$C_{power,min} = \frac{\frac{C_{mem} A}{L_{mem}} + C_{other}}{Capacity} \qquad [24]$$

The EIA published estimates of the cost of electricity generated by U.S. plants expected to enter

service in 2019 in the 2014 Annual Energy Outlook. Various generation methods were analyzed

with the results summarized in Table 6. The average cost for all of the technologies is around

$0.10/kwh.

Table 6. Electricity costs by production method, adapted from EIA report [38]

Plant Type	Levelized Cost of Electricity (cents/kWh)		
	Minimum	Average	Maximum
Conventional Coal	8.70	9.56	11.44
Conventional Natural Gas (Combined Cycle)	6.11	6.63	7.58
Natural Gas (Advanced Combustion Turbine)	9.69	10.38	11.98
Nuclear	9.26	9.61	10.20
Biomass	9.23	10.26	12.29
Wind	7.13	8.03	9.03
Solar (Photovoltaic)	10.14	13.00	20.09
Hydroelectric	6.16	8.45	13.77

In comparison, the current electricity cost in the Gambia is approximately $0.26/kWh due to the inefficient and outdated generation technology currently in use. The effect of this relatively high price discourages economic growth and presents barriers to the adoption of electricity by people living below the poverty line, who make up nearly half of the population. Therefore, PRO could be competitive at $0.26/kWh in the Gambia, but to truly transform the country, the goal for any new generation technology should be around $0.10/kWh.

4.3 Results for Current Membrane Technology

The current best membrane technology for PRO is described by Yip et al. [27]. Although reverse osmosis (RO) membranes are currently much more mature in their level of development, the high operating pressures (typically around 40 bar) require that these membranes have substantial mechanical strength. This is achieved by having thick support layers that cause severe internal concentration polarization, which greatly limits water flux in PRO applications [27]. The Statkraft PRO plant in Norway initially used cellulose acetate membranes which experienced less internal concentration polarization, but the lower intrinsic permeability of cellulose acetate led to power densities less than 0.5 W/m^2 [27]. Therefore, the opportunity still exists for significant improvement of membrane properties for PRO applications that operate at much lower pressures.

The current best practice described by Yip et al. is to use special thin film composite (TFC) membranes with a highly permeable polyamide active layer and a polysulfone support layer [27]. The active layer can be modified to increase water permeability by exposure to

chlorine, although the increase in water permeability must be balanced by the increase in salt

permeability (k_S). Yip et al. prepared a series of membranes using low, moderate, and high

chlorine treatments, giving membranes with properties shown in Table 7 [27].

Table 7. Current PRO membrane characteristics [27]

Membrane Preparation	k_P L / m² hr bar	k_S L / m² hr	S μm	PD_{max} W / m²
Low Permeability	1.63	0.11	349	5.79
Medium Permeability	4.35	0.76	340	9.21
High Permeability	7.55	4.48	360	6.23

The performance of these three membrane types were tested in the PRO cost model to

determine their break-even electricity cost. The medium permeability membrane had the best

overall performance, leading to a break-even energy cost of $0.30/kWh at a permeate fraction of

0.8. In contrast, the low permeability membrane had a break-even energy cost of $0.52/kWh

while energy cost of the high permeability membrane was $0.39/kWh. The key variable in this

analysis is the average water flux, given by Equation (10), which accounts for the effects of both

internal and external concentration polarization. The value of the water flux determines the

required membrane area and the bulk of the operating costs for the PRO plant. The low

permeability membrane has a low water flux due to the greater resistance of the membrane,

while the large value of k_s for high permeability membrane lowers the driving force for water

permeation due to the effects of internal concentration polarization.

Cost of Electricity Generation by PRO with Current Membrane Technology
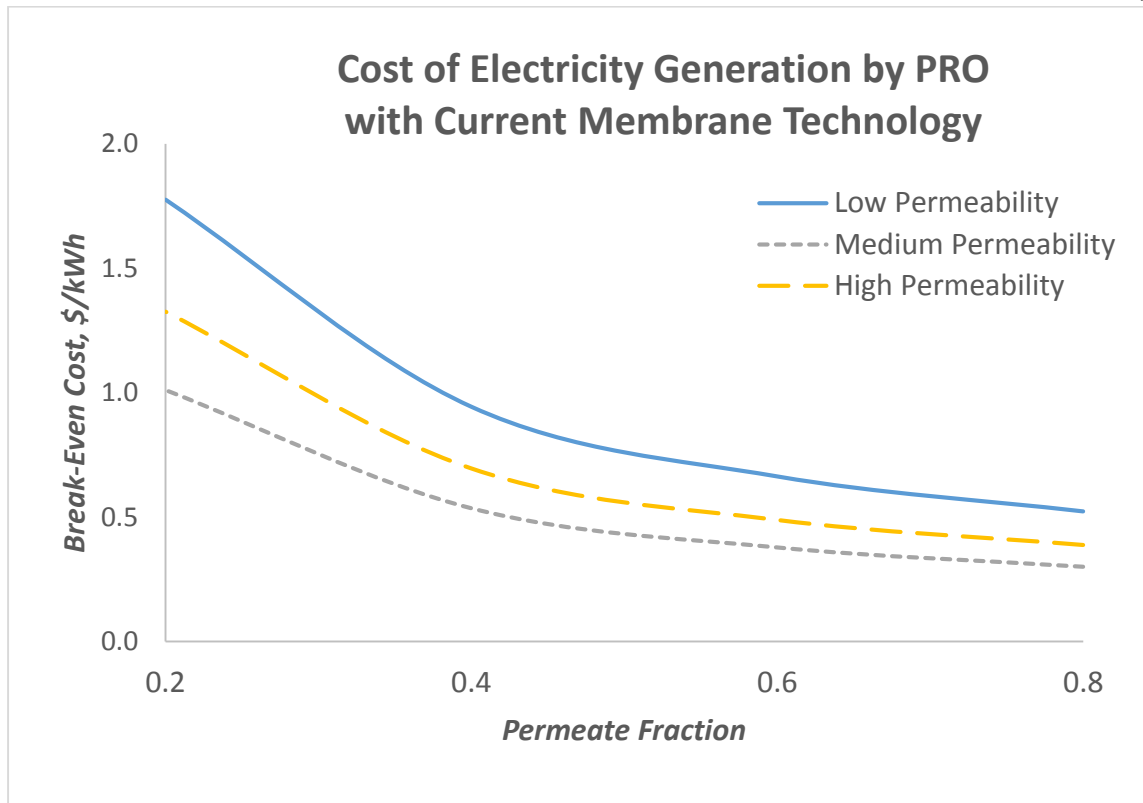
Figure 16: Cost analysis of currently available membranes
c_{f0} = 1mM, c_{d0} = 696 mM, Q = 10 m^3/s, Feed Ratio=0.5, $\$_{mem}$= \$30/m^2, L_{mem} = 3 years

Despite the significant recent advances in membrane technology, even the best currently available membranes require an electricity price greater than \$0.30/kWh to be economically competitive. This cost is about 20% higher than the current price of electricity in the Gambia (\$0.26/kWh) and it is three times greater than the target electricity price of \$0.10/kWh. Further improvements in membrane performance are needed before PRO technology can become a viable competitor in the Gambian energy landscape.

4.4 Sensitivity Analysis

In an effort to examine the key factors governing the overall economic viability for PRO, along with the greatest opportunities for further development, a sensitivity analysis was conducted on the five most important membrane performance and cost variables. The following base case parameters were used in all calculations unless otherwise noted. For each permeate fraction, the optimal operating pressure was determined with values given in Table 4.

Table 8. Base case values for sensitivity analysis

Parameter		
C_{F0}	1	mM
C_{D0}	696	mM
K_P	5	$L\ m^{-2}\ hr^{-1}\ bar^{-1}$
K_S	1	$L\ m^{-2}\ hr^{-1}$
S	307	μm
C_{mem}	30	$\$ / m^2$
L_{mem}	3	years

For the case of an "ideal" membrane with infinite permeability, infinite selectivity, and zero cost, the cost of electricity produced by PRO falls below \$0.03/kWh, which is much smaller than the target of \$0.10/kWh. The sensitivity analysis shows the effect of membrane non-idealities and also examines how improvement may bring the technology closer to the ideal case.

Membrane Water Permeability

All other things being equal, the greater the water permeability of the membrane, the greater the water flux. As a result, the power density is increased and less membrane area is

required to process the same permeate volume. Figure 17 depicts the dependence of the break-even cost on the membrane permeability.

Effect of Membrane Permeability

(Legend: Permeate Fraction = 0.2, Permeate Fraction = 0.4, Permeate Fraction = 0.6, Permeate Fraction = 0.8)

Y-axis: Break-Even Cost, $/kWh

X-axis: Membrane Permeability, L m^{-2} hr^{-1} bar^{-1}
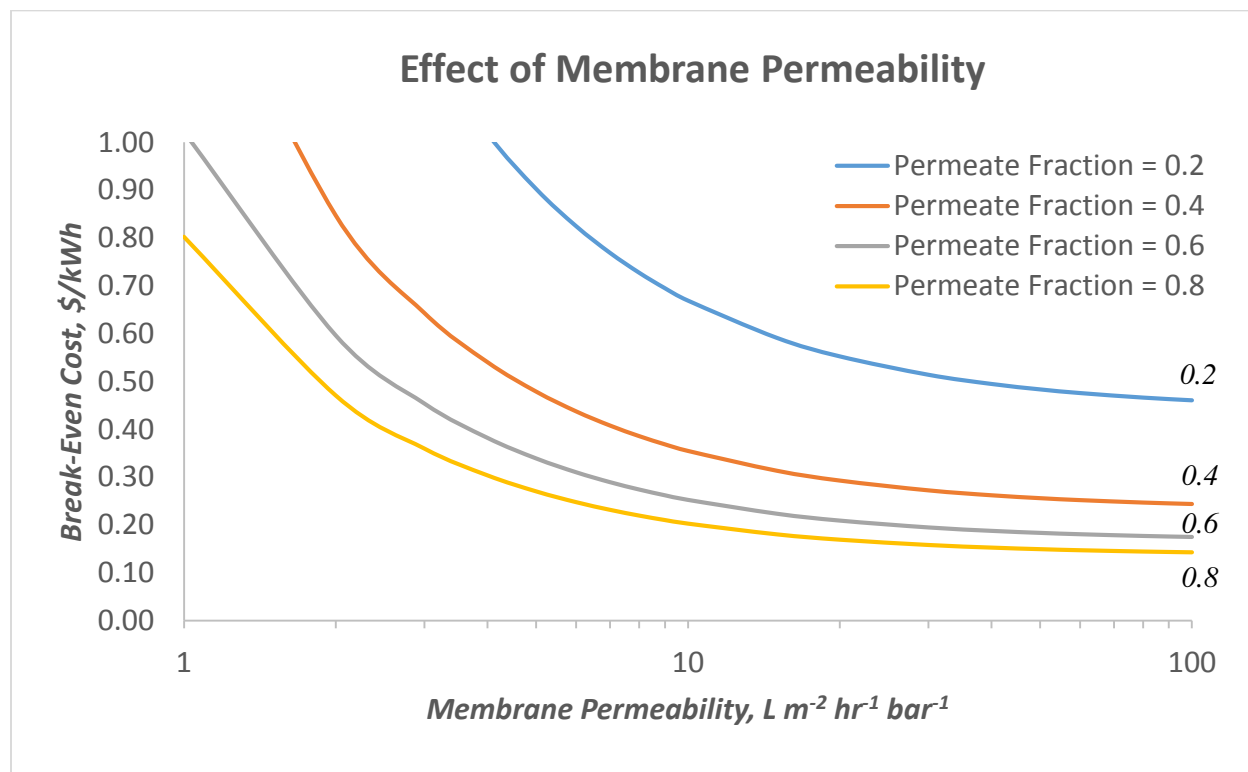
Figure 17: Break-even cost vs. membrane permeability

The break-even cost of electricity decreases rapidly with increasing membrane permeability for small values of k_p, but then begins to level off above a permeability of about 10 L m^{-2} hr^{-1} bar^{-1}. For example, the break-even cost drops by \$0.06/kWh as the membrane permeability increases from 3 to 4 L m^{-2} hr^{-1} bar^{-1}, which is the same reduction in cost seen in going from a permeability of 10 to 100 L m^{-2} hr^{-1} bar^{-1}. At very high permeabilities, the break-even cost approaches a constant asymptotic value determined by the other costs for energy production, with the membrane cost becoming negligible under these conditions. However, it is

important to note that this analysis does not account for the trade-off between the membrane

permeability and selectivity—as permeability increases, the selectivity will typically decrease

(i.e., the solute permeability will increase). Based on the results in Figure 17, a water

permeability of around 10 L m^{-2} hr^{-1} bar^{-1} is likely to be optimal, which leads to a break-even

cost around $0.20/kWh.

The effect of the water permeability on the required membrane area is shown in Figure

18. The membrane area decreases with increasing permeability and decreasing permeate

fraction. For example, in order to achieve a permeate fraction of 0.8 requires approximately 4.5

times the membrane area as a permeate fraction of 0.2.
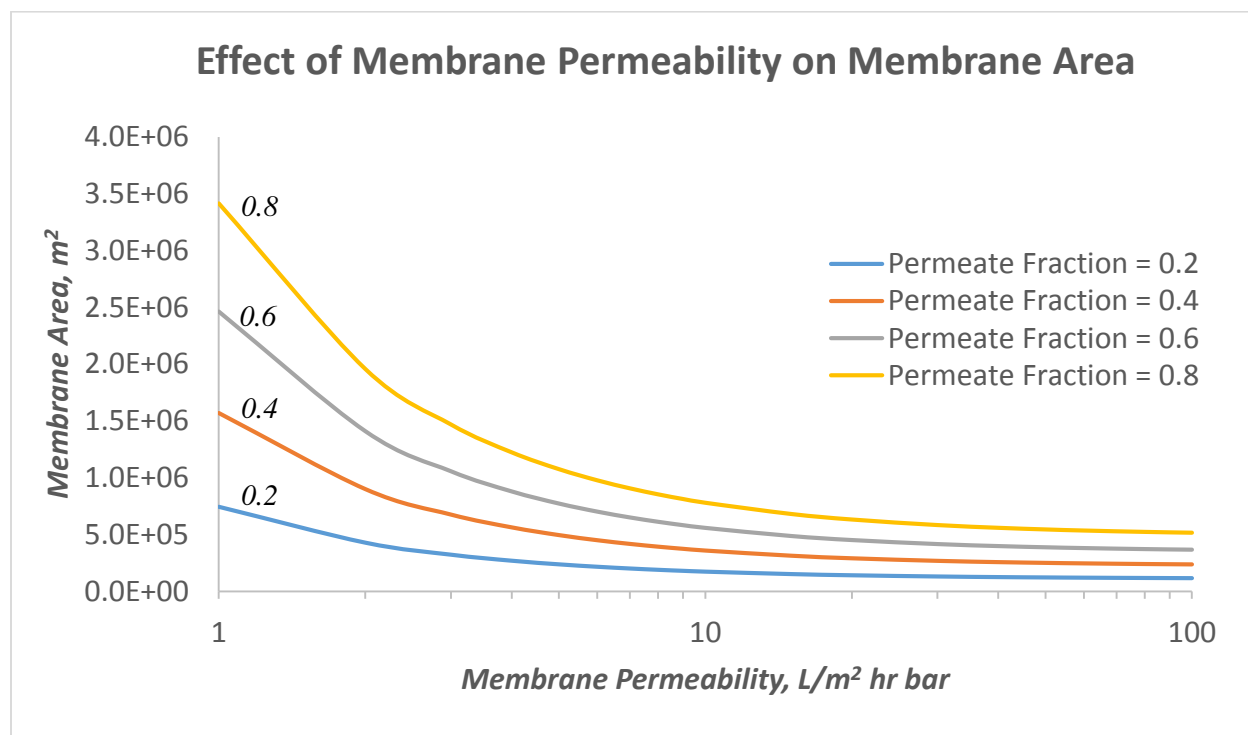
Figure 18: Membrane area vs. membrane permeability

Membrane Salt Rejection

The effect of the salt permeability on the break-even cost is shown in Figure 19. Increasing the salt permeability reduces the water flux thereby decreasing the power that can be extracted from a given volume of water.

Effect of Salt Permeability

0.2

0.4

0.6

0.8

Permeate Fraction = 0.2
Permeate Fraction = 0.4
Permeate Fraction = 0.6
Permeate Fraction = 0.8

Break-Even Cost, $/kWh

Salt Permeability, L/m² hr
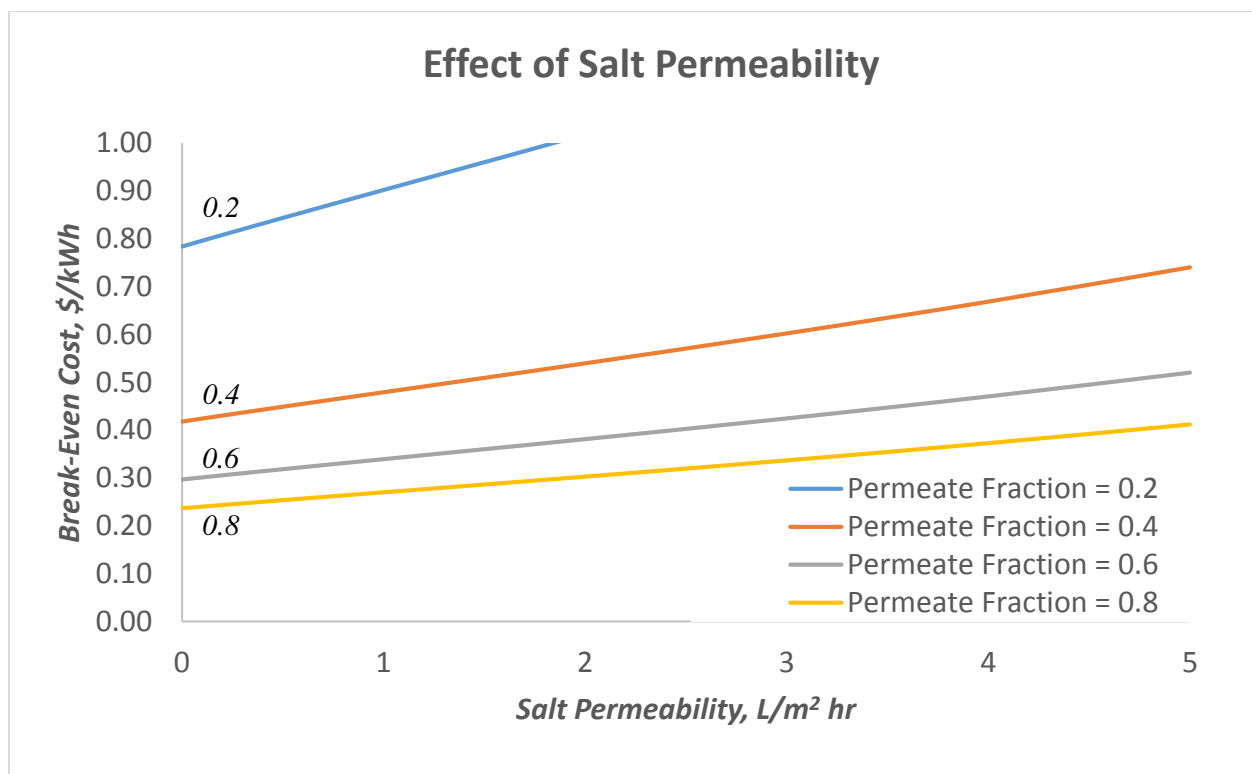
Figure 19: Cost sensitivity vs. membrane salt permeability

The dependence of the break-even cost on the salt permeability is much less pronounced than the effect of the water permeability, particularly for simulations with a large value of the permeate fraction. At high permeate fractions, the average membrane flux is smaller which reduces internal concentration polarization. Note that reducing the salt permeability to 0 from the current

value of 1 L/m^2/hr would have relatively little effect on the overall economics, providing only a

$0.03/kwh reduction in the break-even cost at a permeate fraction of 0.8.

Structural Parameter

The membrane structural parameter controls the extent of internal concentration

polarization and thus the water flux. As shown in Figure 20, the break-even cost increases with

increasing values of the structural parameter due to the increase in internal concentration

polarization and the corresponding reduction in the effective driving force and thus the water

flux. This effect becomes more pronounced at large values of the structural parameter and at

smaller values of the permeate fraction. Similar to the results with the salt permeability (Figure

19), reducing the structural parameter to 0 (from its current value of 307 µm) causes only a 12%

reduction in the break-even cost.
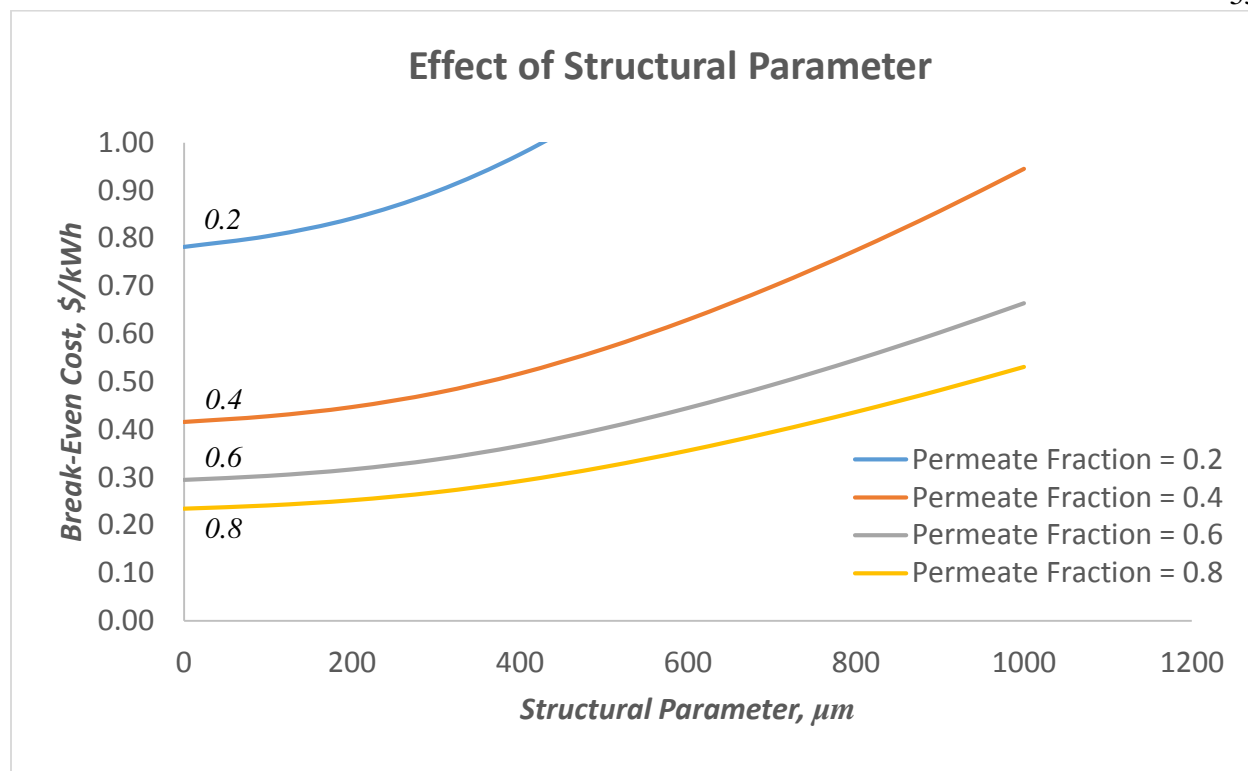
Figure 20: Break-even cost sensitivity vs. structural parameter

Membrane Price

The membrane price has a very large effect on the break-even cost since the membranes contribute over 80% of the total cost of the PRO plant. The break-even cost increases linearly with the membrane price, with the slope being greatest at the lowest permeate fraction. In the limit of zero membrane cost, the break-even cost becomes essentially independent of the permeate fraction due to the assumptions made for estimating the capital and operating costs of the plant. Decreasing the membrane price from its current value of $30/m^2 significantly reduces the break-even cost. For example, a membrane price of approximately $9.10/m^2, which is slightly less than one-third of the cost of today's membranes, gives a break-even cost of $0.10/kWh at a permeate fraction of 0.8. Although this is well below current estimates of

membrane costs, one would certainly expect some reduction in the price of membranes due to economies of scale if large PRO installations were to be constructed. To match current Gambian energy prices, a membrane price of approximately $28.50/m^2 gives a break-even cost of $0.26/kWh at a permeate fraction of 0.8.

Effect of Membrane Cost
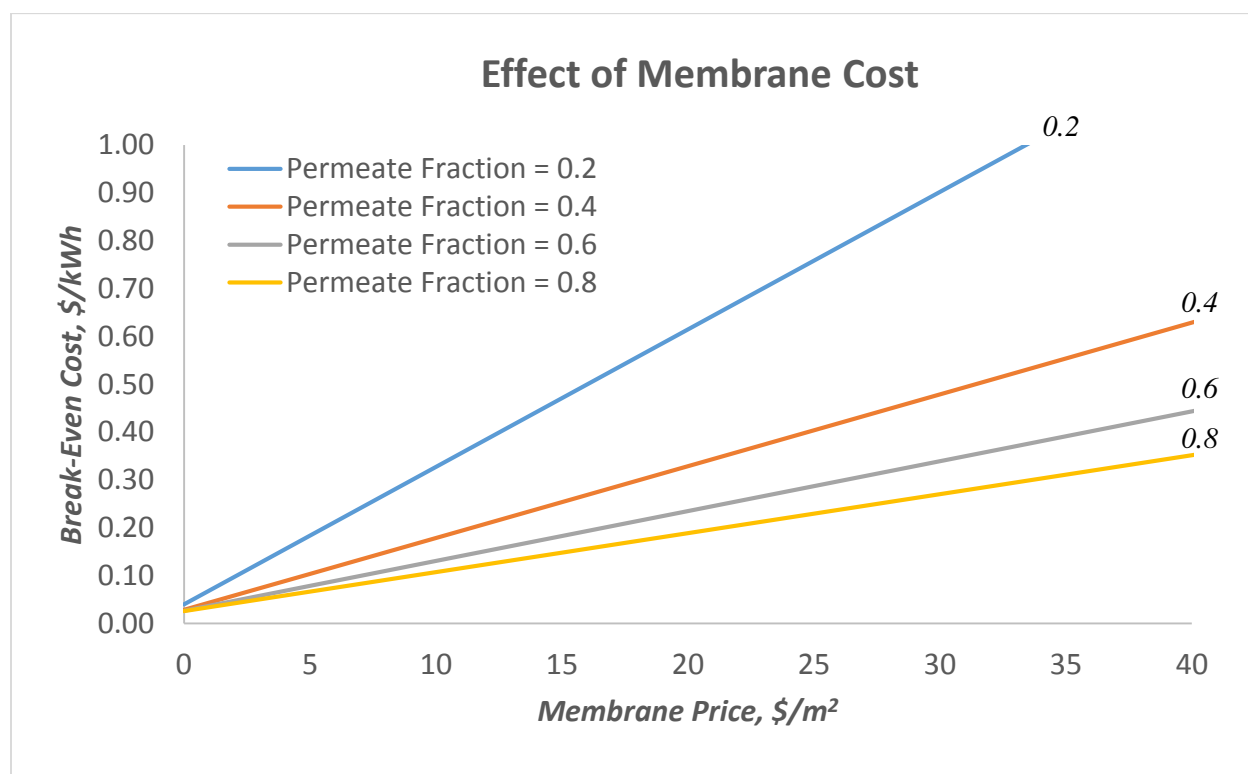
Figure 21: Break-even cost vs. membrane price

Membrane Life

Another approach to decreasing the effective membrane cost is to increase the expected membrane life, reducing the frequency of membrane replacement. Membrane life is determined in large part by the fouling characteristics, which are discussed in more detail in Section 4.5.

The break-even cost initially decreases rapidly with increasing membrane life particularly when

the membrane life is less than three years. However, the incremental benefits decrease as the

membrane life increases much above 5 years. For example, increasing membrane life from 2 to

3 years decreases the break-even cost by 12-43 cents/kWh depending on the permeate fraction,

but the decrease is only 2-8 cents/kWh when the membrane life is increased from 5 to 6 years.

Figure 22: Break-even cost vs. membrane life

Summary

     Based on the results in the previous section, the most important variables controlling the

break-even cost for the PRO system are the membrane cost, the membrane permeability, and the

membrane lifetime, all of which decrease the contribution of the membrane to the overall

operating costs. The greatest benefits are seen with a reduction in the membrane cost, with a

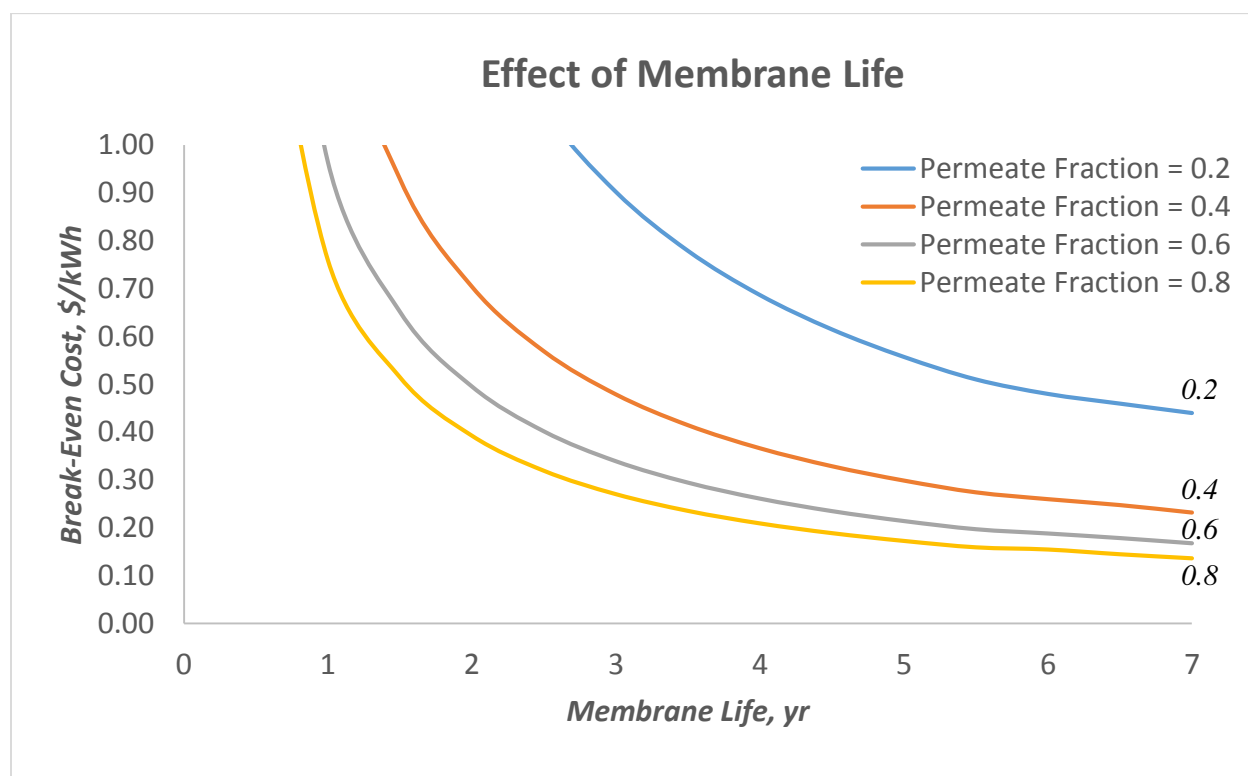price of $9.1/m^2$ yielding a break-even cost of $0.10/kWh. A combination of a reduced

membrane cost with improvements in membrane permeability and membrane lifetime would

provide even further reductions in the break-even cost, possibly making PRO much less

expensive than existing energy generation technologies in the Gambia and highly competitive

with existing energy costs in the U.S.

4.5 Fouling and Pretreatment

One of the most important limitations of membrane processes is the issue of membrane

fouling. This can include clogging of the membrane modules by particulate matter, scale

formation on the membrane surface due to retained inorganic components (e.g., calcium and

silica), and biofilm formation due to deposition of natural organic matter and subsequent growth

of microorganisms. Essentially, membrane fouling has three effects on membranes. First,

fouling reduces the intrinsic water permeability over time. Second, cleaning cycles are needed to

regenerate the membranes to try to restore the baseline permeability. Membrane cleaning

requires energy, time, and typically the use of cleaning chemicals. Finally, repeated cleaning

cycles reduce the effective membrane lifetime. Uncontrolled fouling can also increase the

frictional pressure losses and reduce the turbine efficiency.

All PRO systems will require periodic membrane regeneration cycles that are triggered

when the membrane permeability drops below a certain lower limit. This lower limit depends on

the physical characteristics of the membrane, e.g., the initial permeability, and the detailed plant

operating costs. The sensitivity analysis presented in the previous section assumed that k_p was

equal to the time-averaged permeability over a cleaning cycle, which should provide a reasonable estimate of the costs even in the presence of fouling. However, the model did not account for the loss in operating time during the cleaning cycle.

Fouling is likely to be a significant challenge in the Gambia. River water and seawater contain particulate matter, scale-forming compounds, and biofilm-forming microorganisms. Some sort of pretreatment steps would thus be necessary to protect the PRO membranes and other equipment from fouling, requiring additional capital investment. The key question is how much up-front capital would need to be deployed to mitigate the ongoing costs of fouling.

Particulate fouling can be mitigated using conventional filtration prior to the water entering the PRO system. Coarse debris such as plant matter and wildlife can be eliminated easily and inexpensively through weirs and bar-screens on the water intakes [20]. Removing suspended solids requires further separation. Fortunately, the Gambia River carries a relatively low sediment load as a result of its armored bottom and low flow rate during the dry season [39]. Total suspended solids (TSS) vary based on river flow rate, geometry, and sampling location, with averages of 45 mg/L in the upper river section, 25 mg/L in the lower river section, 75 mg/L in the upper estuary section, and 84 mg/L in the lower estuary section [39]. However, despite a relatively low solids load, a flow rate of 10 m^3/s with a TSS content of 75 mg/L will carry 0.75 kg/s of sediment into the PRO system. A large portion of this sediment needs to be removed prior to entering the membrane module. Particle size distribution analysis should be carried out to determine the filtration level required to remove sufficient levels of solids, but a reasonable starting point is a 50 μm cut-off filter, which is what was used at the Statkraft PRO plant [20, 29].

Post [20] conducted a preliminary comparison of separation processes to determine the most efficient and cost effective method for feed pretreatment in a PRO system. This included filtration, settling, decanting, centrifugation, cyclone separation, flotation, elutriation, flocculation, and biological treatment. Mechanical filtration through microscreen filters was concluded to be the best current option based on its low cost, low energy requirement, and relatively minor system footprint [20]. As a significant quantity of solids will need to be removed, a micro-screen rotating drum filter or similar setup is recommended. The micro-screen mesh allows water to pass through the drum radially while trapping solids that are too large to pass through the mesh. As the mesh becomes loaded with solids, it rotates out from the water flow path and passes in front of backwashing nozzles which use a small quantity of high-pressure water to wash the solids off of the screen into a discharge collection system. This setup enables mechanical filtration with no downtime required to change filter elements, which would be a significant cost if using a bag or cartridge type filter system. According to Post, the capital cost of a rotating drum filtration system that can handle 1 m^3/s of water is on the order of $1 million [20]. It was assumed that the cost of this filtration system is captured in the cost of mechanical equipment for the plant. Detailed process data would be required to generate a more accurate cost estimate for the filtration system needed for the PRO plant.

Scale is most commonly composed of calcium carbonate and calcium sulfate that precipitates out of the liquid phase onto the membranes when the concentration of these compounds exceeds the solubility limits [40]. This typically occurs due to external concentration polarization caused by the membranes— the rejected ions accumulate near the membrane surface causing the local salt concentration near the membrane to be much higher than the bulk ion concentration. Scale leads to reduced membrane flux and increased membrane pressure drop,

both of which are detrimental to energy production through PRO. Scale inhibition is typically accomplished through pH control and / or the use of anti-scalant additives, the most common of which are polymeric organic compounds that are added to the feed water to impede nucleation and crystal growth of the scale compounds [40]. Proper use of these additives can effectively control scale formation, but careful study would need to be conducted to determine to verify that the presence of these compounds in the plant discharge would not cause any adverse effects to the river ecosystem.

Biofouling is the last significant challenge facing a PRO plant on the Gambia River. For most membrane systems, the single largest contributor to membrane flux decline is biofilm accumulation [41]. Typically, biofouling in industrial cooling water systems is managed through chlorination or the use of other biocides. However, since the discharge of the PRO plant will need to be routed back to the river, adding biocides should be discouraged to minimize effects on the river ecosystem. A more promising approach was taken by Kim et al. [41] by incorporating titanium dioxide nanoparticles in the polyamide layer of the thin film composite (TFC) membranes. A photobactericidal effect occurred when the hybrid membrane system was illuminated with UV light, resulting in substantial reduction in biofouling [41]. Further analysis and testing should be carried out to determine the effectiveness of this system for inactivation of microorganisms from the Gambia River, and a cost-benefit analysis should be conducted to evaluate the tradeoff between decreased biofouling and increased membrane cost due to the titanium dioxide.

The initial cost estimates developed in this study only considered fouling through the assumed 95% availability factor in the plant capacity calculations. If fouling is a significant problem, the availability factor will decrease as more time would be required for membrane

cleaning cycles. Figure 23 shows the effect of lost power production due to fouling, where the

fouling factor is defined as the fraction of the total time in which the plant is in operation (i.e.,

producing power). This analysis does not account for the increased labor costs associated with

high fouling rates, e.g., the additional staff required to conduct the cleaning. In addition, the

membrane lifetime was assumed to be independent of the fouling. Thus, the results in Figure 23

will underestimate the actual costs of fouling in a PRO system.
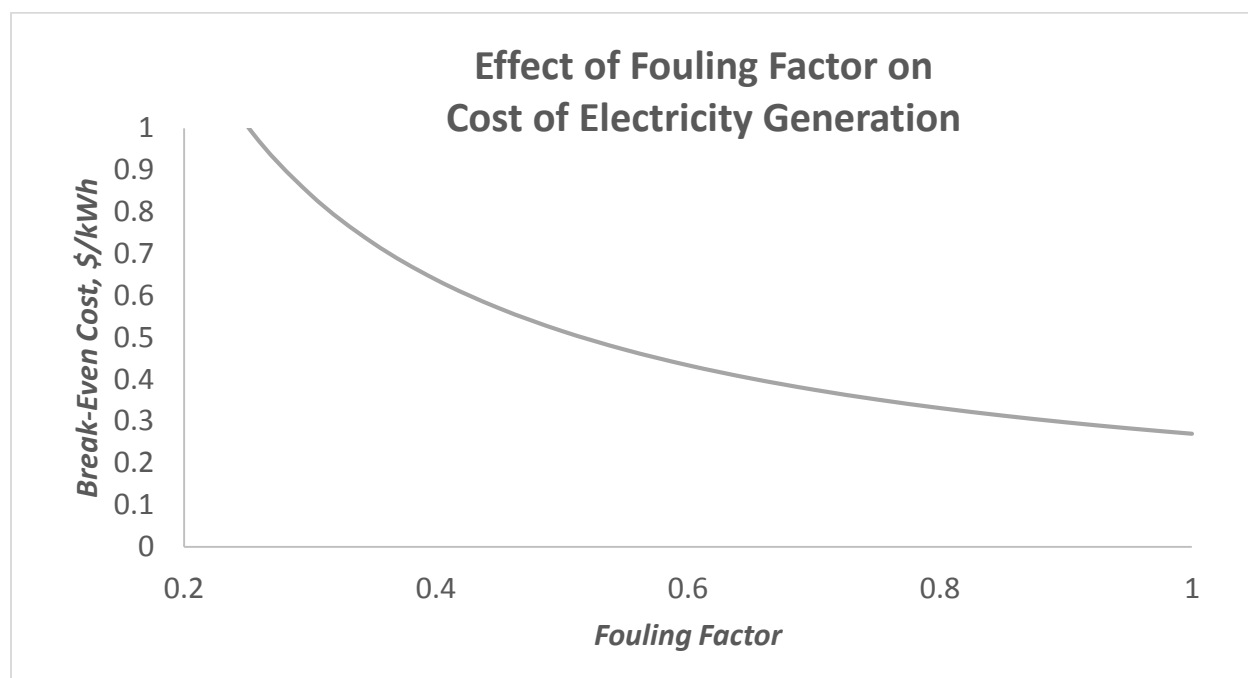

Figure 23: Effect of fouling factor on cost of electricity generation

With 100% plant availability, the break-even electricity cost for the base case is

$0.27/kWh. Between 50% and 100% availability, the cost change is nearly linear, with the

break-even price almost doubling to $0.52/kWh at 50% availability. The break-even cost

increases rapidly at smaller values of the fouling factor, although such small values of the fouling

factor are unlikely to be encountered in a real PRO facility.

4.6 Variations in Flow and Salinity

The river flow rate is a critical parameter governing the performance of any salinity

gradient power plant because the amount of power generated is directly proportional to the

volumetric water flow rate through the membrane, which is limited by the feed rate of the river.

The Gambia River is fed by rainfall in the Gambia River Basin, which covers approximately

77,000 km^2 of land across Guinea, Senegal, and the Gambia [33]. The semitropical climate of

the Gambia consists of a rainy season from approximately May to October and a dry season for

the remainder of the year. This cycle of precipitation leads to peak flows on the order of 1000-

1500 m^3/s from August to October but very low baseline flows for the remaining 9 months of the

year, with flows typically averaging 10-100 m^3/s and reaching minimums of 2-3 m^3/s [18].

Target baseline flows are 20 m^3/s after the Sambangalou Dam is commissioned, which is

projected to occur in 2018 [33]. For perspective, the largest reverse osmosis plant in the world is

the Sorek plant in Israel which produces 7.2 m^3/s (624,000 m^3/day) [42]. Therefore, the fresh

water flow rate would not be expected to be a limiting factor in power production.

The flow variations also indirectly impact the power generation capability by causing

variations in the salinity of the fresh water feed stream. Although the flow rate is sufficient, the

variability in salt content of the fresh water feed could be a major technical obstacle for a PRO

plant in the Gambia.

During periods of high flow, the transition from fresh water to salt water occurs rapidly at the mouth of the river. A phenomenon known as a saline wedge can occur, where lighter fresh water flows over denser salt water [33]. During low flow periods, the separation between fresh water from the river and saline water from the sea is not clearly defined in the estuary. Tidal influence and dispersion effects cause salt to be transported upriver, forming a salinity gradient which decreases from 35 g/L at the river's mouth to less than 0.1 g/L at the head [33]. The extent of this intrusion depends mainly on the fresh water flow rate and the geometry of the estuary. In the case of the Gambia River estuary, the extremely flat terrain means that tidal influences can be observed even up to 500 km inland during periods of very low flow [33]. As a result, saline intrusion can be significant, especially during the dry season. This effect is exacerbated by fresh water abstraction for irrigation and domestic consumption. Typical variations in flow and salinity are shown in Figure 24.
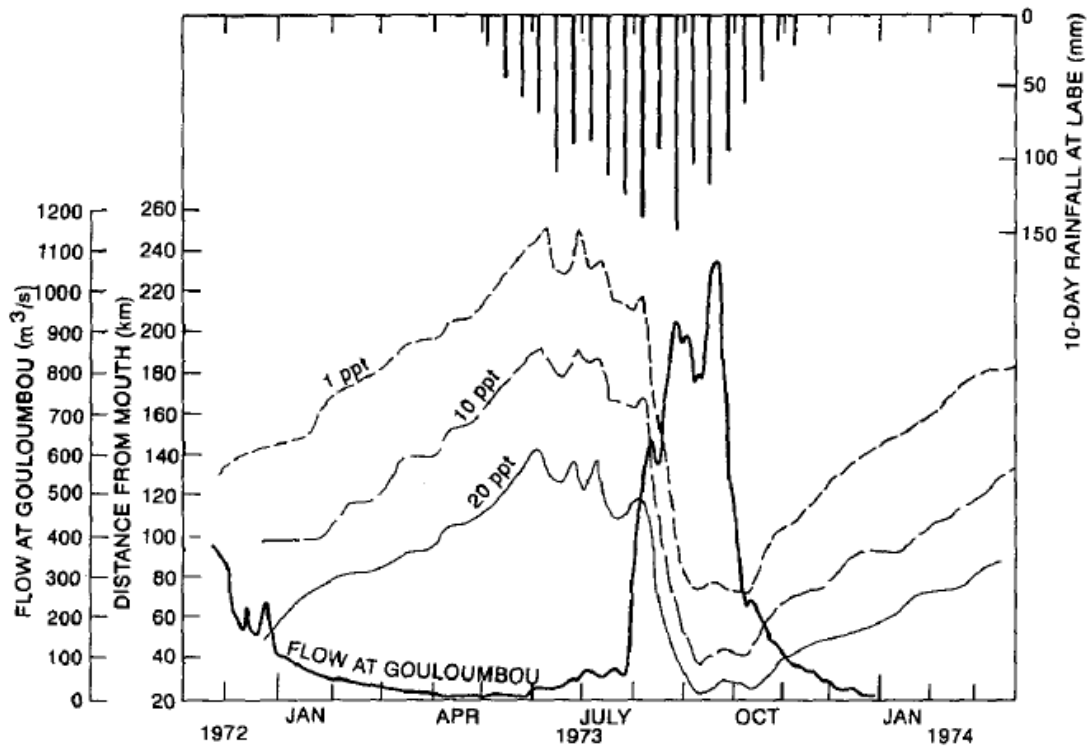
Figure 24: Annual rainfall, river flow, and salinity intrusion in estuary [33]

The Gambia River is one of the last major rivers in Africa that has not been dammed. Therefore, the data collected in the 1970's is still representative of river behavior as the river remains free-flowing to this day. Figure 24 includes three sets of data: rainfall measurements at Labe (in the upper river basin), flow data from the Gouloumbou station, and movements of three different salinity fronts (in parts per thousand) along the course of the river. The Gouloumbou station, near the border of Senegal and the Gambia, is the official beginning of the Gambia River estuary and the benchmark for Gambia River flow data. The figure shows a strong relationship between upper basin rainfall, fresh water flow, and salinity levels along the river. After a lag period, flow increases as a result of rainfall, which flushes saline water out of the estuary towards the ocean. These seasonal variations in salinity can be seen in Figure 25.
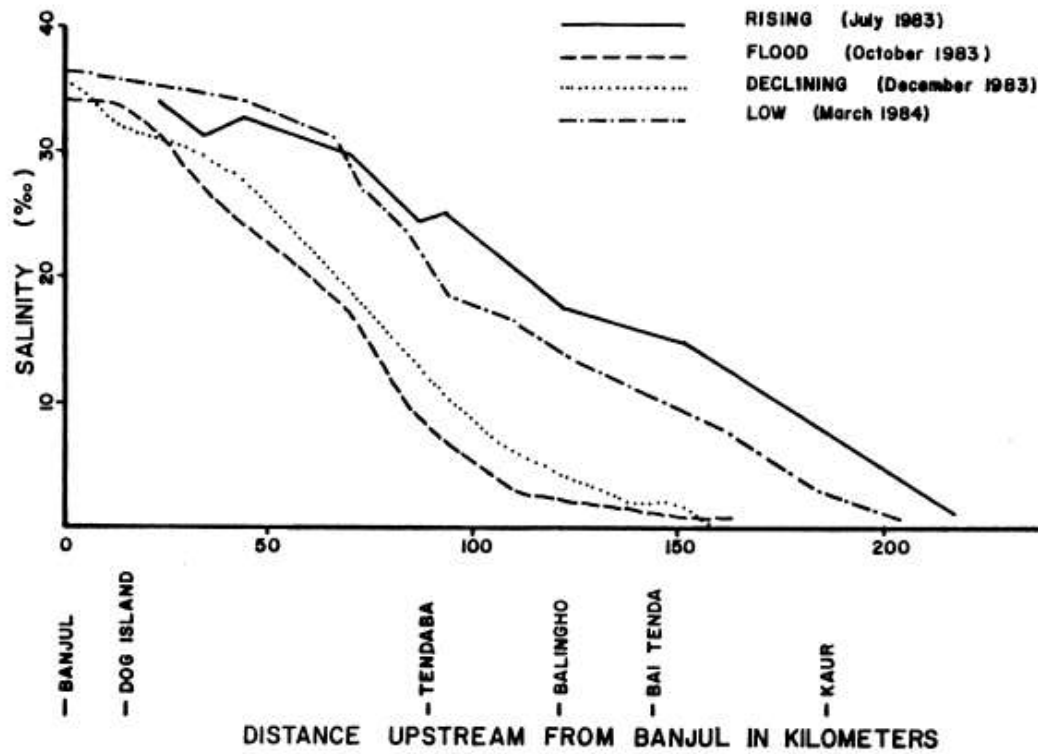
Figure 25: Salinity of the Gambia River in various stages [39]

During the low flow period in the dry season, the salinity gradient is very gradual, averaging a change of 0.17 parts per thousand per kilometer (ppt/km) [39]. During flood stage, the gradient is steeper, averaging 0.40 ppt/km, but securing sources for feed and draw solutions with meaningful differences in salinity would still remain a challenge. The effect of feed salinity on the break-even cost is shown in Figure 26. In this analysis, the base case membrane characteristics were used and the feed salinity was increased. In addition to changing the feed salinity input in the model, the available energy from mixing and efficiency were also changed to match the values in Table 3. The optimal pressure analysis was repeated to get new optimum operating pressures for both 1 mM and 20 mM salinity.

Effect of Feed Solution Salinity
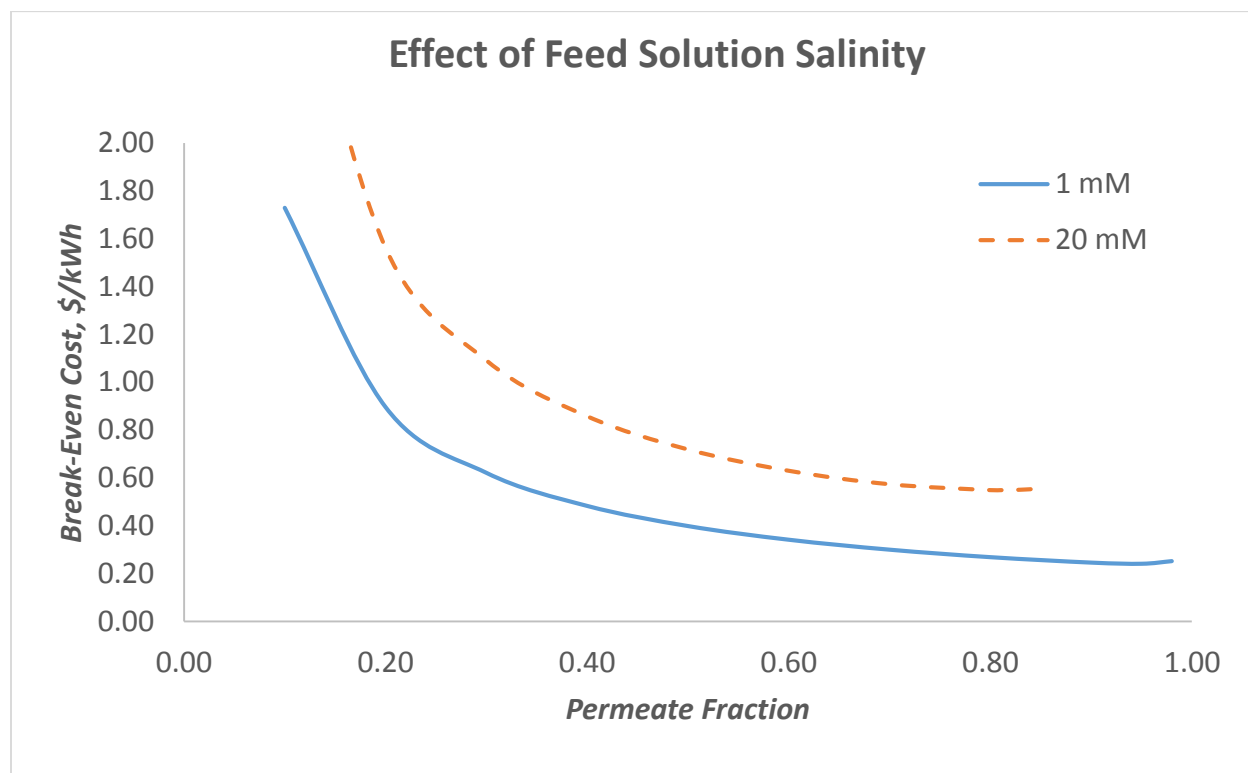
Figure 26: Effect of increased feed salinity on power cost

An increase in feed salinity from 1 mM (0.05 ppt) to 20 mM (1 ppt) more than doubles the break-even cost, from \$0.25/kWh to \$0.55/kWh. Additionally, this increase in salinity meant that permeate fractions larger than 0.85 are not attainable; at this point, the osmotic pressure of the concentrated feed water is equal to that of the seawater. Further increases in feed salinity lead to even greater increases in the break-even cost — a feed with a salinity of 200 mM (10 ppt) would have a break-even cost greater than \$5/kWh even at the highest possible permeate fraction due to the reduction in the available energy of mixing coupled with reductions in operating efficiency and the maximum achievable permeate fraction.

Modern salinity gradient power plants in Norway and the Netherlands were built in regions where there is a very rapid transition from fresh water to salt water. In Norway, the natural geography of the fjords creates significant elevation differences that inhibit saltwater intrusion. The Netherlands does not have any natural elevation differences, but hundreds of years of hydraulic engineering projects have significantly altered the natural flow of the Rhine River and nearly doubled the land area of the country. One of the most significant engineering projects is the Zuiderzee Works, a major system of dikes completed in 1932 [43]. This project transformed the Zuiderzee, at the time a dangerous inlet of the North Sea, into the calm fresh water lake IJsselmeer, which is now the largest lake in Western Europe. As a result of this massive project, there is a man-made barrier that separates the fresh water reservoir and the sea.

In contrast, the Gambia River is almost a worst-case scenario for PRO. A long, flat, wide estuary with relatively low flow for most of the year means that mixing takes place gradually along the entire estuary rather than at a single point. Securing a source of fresh water with consistently low salt content would require a major civil engineering project.

Saline intrusion in the Gambia River has historically been a problem for agriculture on the banks of the Gambia River, especially rice farmers, because salt water is detrimental to crop health [18]. In the 1980's, a dam construction project was proposed in order to halt upstream movement of saline water and to create a fresh water reservoir for irrigation. However, the project was canceled after an environmental impact study showed that building a dam would reduce the mangrove area, detrimentally affect the coastal fishing industry, increase coastal erosion, and increase risk of lethal waterborne illnesses such as malaria and bilharzia [2]. Until these challenges are overcome, the feasibility of salinity gradient power generation in the Gambia is likely to be very limited.

Chapter 5

Concluding Remarks

Salinity gradient power generation offers the potential for a continuous, local, and renewable source of energy in any place with a river estuary. This analysis considered the short-term and long-term viability of this technology in the Gambia River estuary system.

The short-term viability of this technology, both in the Gambia and in other regions around the world, is limited mainly by the current market landscape and the economics of the PRO process. To compete with other major energy generation technologies, the electricity price needs to be on the order of $0.10/kWh (unless major government subsidies are provided). This price is out of reach based on current membrane technology and prices, in particular the membrane cost, the water permeability, and membrane life. Model simulations with a membrane cost of about $9/m^2 would yield an electricity price of $0.10/kWh for a PRO system (assuming current values for the membrane properties and lifetime). This is less than a third of current membrane prices, even for large-scale reverse osmosis operations. Significant improvements in membrane performance and cost would thus be required before this technology becomes competitive with alternative energy generation technologies.

The long-term viability of PRO technology in the Gambia would likely be limited by access to water with a reasonably low salt concentration. The geography of the river estuary results in significant salinity intrusion, dramatically reducing the effectiveness of the energy extraction technology. It would be possible to create a man-made salinity barrier in the Gambia River, but concerns over environmental impact would need to be addressed before this could be implemented. PRO power plants could be more promising for other estuary systems where salinity intrusion is not as prevalent.

Even if these obstacles were overcome, the relative scale of the technology would be a challenge. Based on current estimates, a 5 MW PRO plant in the Gambia would have a footprint on the order of 100,000 m^2. This would be equivalent to the area of over 20 American football fields—truly a world-class size facility. However, at average African consumption levels, 5 MW would only provide enough electricity for approximately 75,000 people, or 4% of the population (at current rates of electricity consumption). Diesel or heavy fuel oil generators could produce the same amount of energy with less than a tenth of the footprint and far less capital investment. At this point, the capital investment for a PRO plant would likely be better spent improving the electricity transmission and distribution network, repairing and upgrading current generators, and investigating alternative generation technologies – these would have a much greater impact on providing reliable access to electricity for the Gambian people.

BIBLIOGRAPHY

1. "The Gambia." The World Bank, 2015. *<data.worldbank.org>*

2. Scott, D. B., J. Frail-Gauthier, and P. J. Mudie. *Coastal Wetlands of the World: Geology, Ecology, Distribution and Application*s. Cambridge UP, 2014.

3. "History of the Gambia." Access Gambia, 2015. *<accessgambia.com>*

4. *Human Development Report 2014: Sustaining Human Progress- Reducing Vulnerability and Building Resilience.* United Nations Development Programme. New York: PBM Graphics, 2014.

5. Singh, G., S. A. Nouhou, and M. Y. Sokona. "The Gambia: Renewables Readiness Assessment 2013." (2013). *<irena.org>*

6. Simoes, A. "OEC: Gambia (GMB) Profile of Exports, Imports and Trade Partners." The Observatory of Economic Complexity. *<atlas.media.mit.edu>*

7. "How Much Electricity Does an American Home Use?" *EIA - Independent Statistics and Analysis.* U.S. Energy Information Administration, 20 Feb. 2015. *<eia.gov>*

8. "About Us- Power Generation." National Water & Electricity Company. *<nawec.gm>*

9. Ceesay, A. "Gambia: 20 Years of Energy Sector Transformation."24 July 2014. *<allafrica.com>*

10. "Electricity." Public Utilities Regulatory Authority, 2011. *<pura.gm>*

11. "About Us - Power Transmission." National Water & Electricity Company. *<nawec.gm>*

12. Electricity Act of 2005, The Gambia.

13. "Electricity Tariffs." Public Utilities Regulatory Authority, 2011. *<pura.gm>*

14. Gambia Programme for Accelerated Growth and Employment Report. Ministry of Finance and Economic Affairs, The Gambia, 2011.

15. Renewable Energy Act of 2013, The Gambia.

16. Norman, R.S., Water Salination: A Source of Energy, Science 186 (1974) 350-352.

17. "Hoover Dam FAQs." U.S. Bureau of Reclamation, Dec. 2008. *<usbr.gov>*

18. Risley, J. C. "Salinity-Intrusion Forecasting System for Gambia River Estuary." *Journal of Water Resources Planning and Management* 119.3 (1993) 339-352.

19. "Tidal Irrigation, The Gambia." *Sourcebook of Alternative Technologies for Freshwater Augumentation in Africa.* United Nations Environmental Programme. *<unep.or.jp>*

20. Post, J.W. Blue Energy: Electricity Production from Salinity Gradients by Reverse Electrodialysis. PhD Thesis, Wageningen University, 2009.

21. Yip, N. Y., and M. Elimelech. "Thermodynamic and Energy Efficiency Analysis of Power Generation from Natural Salinity Gradients by Pressure Retarded Osmosis." *Environmental Science & Technology* 46 (2012) 5230-239.

22. Betts, J. G., P. Desaix, E. Johnson, J. E. Johnson, O. Korol, D. Kruse, B. Poe, J. Wise, M. Womble, and K. Young. *Human Anatomy and Physiology*. Rice University, 2014.

23. Morse, H. N. *The Osmotic Pressure of Aqueous Solutions; Report on Investigations Made in the Chemical Laboratory of the Johns Hopkins University during the Years 1899-1913.* Washington, D.C.: Carnegie Institution of Washington, 1914.

24. Helfer, F., C. Lemckert, and Y. G. Anissimov. "Osmotic Power with Pressure Retarded Osmosis: Theory, Performance and Trends – A Review." *Journal of Membrane Science* 453 (2014) 337-358.

25. Yaroshchuk, A. "Optimal Hydrostatic Counter-pressure in Pressure-Retarded Osmosis with Composite/Asymmetric Membranes." *Journal of Membrane Science* 477 (2015) 157-60.

26. Yip, N. Y., D. A. Vermaas, K. Nijmeijer, and M. Elimelech. "Thermodynamic, Energy Efficiency, and Power Density Analysis of Reverse Electrodialysis Power Generation with Natural Salinity Gradients." *Environmental Science & Technology* 48.9 (2014) 4925-4936.

27. Yip, N. Y., A. Tiraferri, W. A. Phillip, J. D. Schiffman, L. A. Hoover, Y. C. Kim, and M. Elimelech. "Thin-Film Composite Pressure Retarded Osmosis Membranes for Sustainable Power Generation from Salinity Gradients." *Environmental Science & Technology* 45 (2011) 4360-4369.

28. Skråmestø, Ø. S., S. E. Skilhagen, and W. K. Nielsen. "Power Production Based on Osmotic Pressure." Statkraft, 2008. *<statkraft.com>*

29. Nielsen, W. K. "Progress in the Development of Osmotic Power." 2011 Quingdao International Conference on Desalination and Water Reuse.

30. "Statkraft Halts Osmotic Power Investments." Statkraft, 20 Dec. 2013. *<statkraft.com>*

31. "Dutch King Opens World's First RED Power Plant Driven on Fresh-Salt Water Mixing." Dutch Water Sector, 26 Nov. 2014. *<dutchwatersector.com>*

32. "Composition of Seawater." *Water Treatment Solutions*. Lenntech. *<lenntech.com>*

33. Verkerk, M. P., and C. P. Van Rens. "Saline Intrusion in Gambia River After Dam Construction." Department of Water Resources, University of Twente (2005).

34. U.S. Energy Information Administration. *Updated Capital Cost Estimates for Utility Scale Electricity Generating Plants.* U.S. Department of Energy, 2013.

35. Zhu, A., P. D. Christofides, and Y. Cohen. "On RO Membrane and Energy Costs and Associated Incentives for Future Enhancements of Membrane Permeability." *Journal of Membrane Science* 344.1-2 (2009): 1-5.

36. "Turbine Costs – Hydro Resource Evaluation Tool." *North West Hydro Resource Model.* Lancaster University. *<engineering.lancs.ac.uk>*

37. Bræin, S., Ø. S. Skråmestø, and S. E. Skilhagen. "Osmotic Power, from Prototype to Industry - What Will It Take?" 3rd International Conference on Ocean Energy, Bilbao. 2010.

38. U.S. Energy Information Administration. *Levelized Cost and Levelized Avoided Cost of New Generation Resources in the Annual Energy Outlook 2014*. U.S. Department of Energy, 2014.

39. Barry, T. D., R. A. Moll, and G. L. Krause. *Physical and Chemical Environment of the Gambia River, West Africa 1983-1984*. Great Lakes and Marine Waters Center International Programs Report Number 9. Ann Arbor, Michigan: U of Michigan, 1985.

40. Tzotzi, C., T. Pahiadaki, S. Yiantsios, A. Karabelas, and N. Andritsos. "A Study of $CaCO_3$ Scale Formation and Inhibition in RO and NF Membrane Processes." *Journal of Membrane Science* 296.1-2 (2007) 171-184.

41. Kim, S. H., S-Y. Kwak, B-H. Sohn, and T. H. Park. "Design of TiO_2 Nanoparticle Self-assembled Aromatic Polyamide Thin-film-composite (TFC) Membrane as an Approach to Solve Biofouling Problem." *Journal of Membrane Science* 211 (2003) 157-165.

42. "World's Largest SWRO Desalination Plant Operational." *Desalination & Water Reuse.* The International Desalination Association, 21 Oct. 2013. *<ide-tech.com>*

43. Krystek, L. "The Zuiderzee and Delta Works of the Netherlands." *The Seven Modern Wonders*. 2011. *<unmuseum.org>*

David Hughes

Current Address
508 S. Fraser St
State College, PA 16801

drh5172@psu.edu
(513) 787-8747

Permanent Address
8082 Kingfisher Lane
West Chester, OH 45069

EDUCATION:

Bachelor of Science in Chemical Engineering   *Graduation: May 2015*
Schreyer Honors College
Minors in Engineering Leadership Development and Spanish
The Pennsylvania State University, University Park, PA

EXPERIENCE:

Field Engineer Intern   May 2014-August 2014
Williams   *Tunkhannock, PA*
- Created a tool that predicts compressor station performance based on operating conditions and equipment constraints to assist with planning, maintenance, and station optimization
- Quantified financial impact of salt contamination to build a business case for mitigation project
- Rotated with Operations, Well Connects, and Instrumentation & Controls groups

Facilities Engineer Co-op   January 2013-August 2013
ExxonMobil   *Beaumont, TX*
- Developed the technical basis for a new feed stream to capture $0.94M/year in additional revenue
- Scoped a filter installation project to capture $1.1M/year in cost savings from increased reliability
- Analyzed 4 years of historical process data and performed over 5,000 engineering calculations to create a report for submission to the EPA
- Led a team of co-op students to create a turnaround inspection information management system
- Designed a mitigation system for high temperature excursion safety hazards on process equipment

Manufacturing Engineer Intern   June 2012-August 2012
Procter and Gamble   *Mehoopany, PA*
- Drove 11 projects to completion on 2 different Charmin production lines
- Created an Excel VBA program that automates downtime data analysis to allow sharper focus on improvement areas and save 1600+ man-hours/year
- Designed upgraded trim removal system to eliminate line stops and reduce waste
- Took on additional safety improvement and waste reduction projects proactively

Undergraduate Research in Chemical Engineering   August 2011-Dec 2011
Dr. Darrell Velegol   *University Park, PA*
- Explored methods to create various oil-water emulsions
- Researched the fluid flow dynamics of emulsions in microchannels
- Explored effects of naturally occurring minerals on flow with application to oil extraction

Associate Engineer- Chemical Intern   May 2011- August 2011
ArcelorMittal   *Coatesville, PA*
- Designed and performed an experiment to evaluate ArcelorMittal rapid austenitization practice
- Proposed a method to achieve an 80% time reduction in austenitization process
- Researched advanced metallurgy related to heat treatment, austenitization, and carbide dissolution

Student Research Chemist   June 2009 – August 2009
USDA Poisonous Plant Research Lab   *Logan, UT*
- Synthesized toxin present in poison hemlock
- Presented findings with mentor at the American Chemical Society National Conference in Washington, DC— August 2009
- Published research in *Chemical Research in Toxicology*— March 2013

ADDITIONAL ACTIVITIES:
- Springfield THON (Pediatric Cancer Philanthropy Organization)   August 2010- Present
- Study Abroad Experience: Granada, Spain   January 2012- May 2012